AC SAF VALIDATION REPORT

Validated products:

Name	Satellite(s)
Near real-time total SO_2	Metop-C

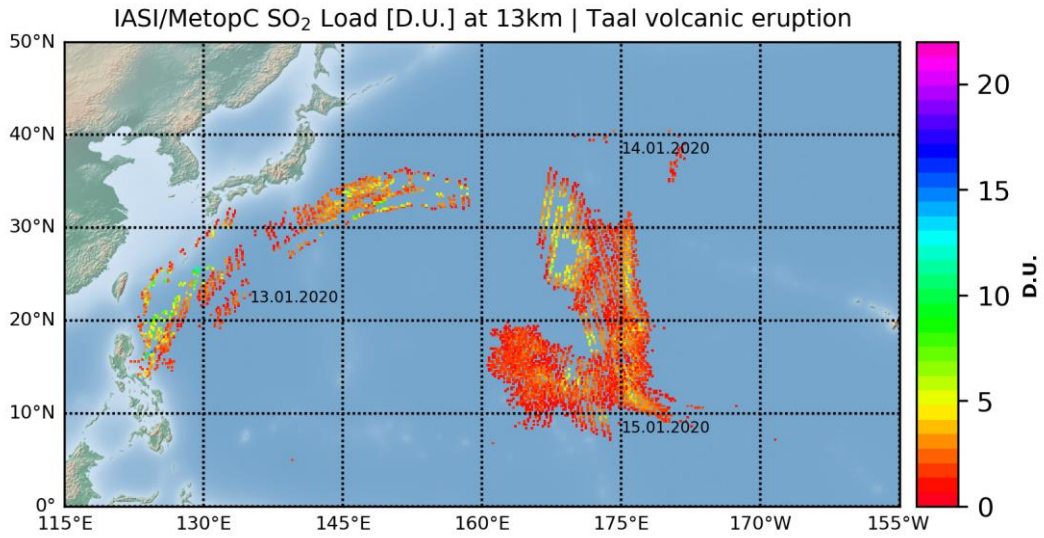

IASI/MetopC reported Sulphur dioxide plume during three days after the Taal Volcano eruption on January 12th, 2020.

Authors:

Name	Institute
MariLiza Koukouli	Laboratory of Atmospheric Physics, Aristotle University of Thessaloniki
Gaia Pinardi	Royal Belgian Institute for Space Aeronomy
Bavo Langerock	Royal Belgian Institute for Space Aeronomy

Reporting period:	September 2019 – March 2021
Input data versions:	IASI/MetopC NRT EumetCAST BUFR
Data processor versions:	Brescia v6.05

Introduction to EUMETSAT Satellite Application Facility on Atmospheric Composition monitoring (AC SAF)

Background

The monitoring of atmospheric chemistry is essential due to several human caused changes in the atmosphere, like global warming, loss of stratospheric ozone, increasing UV radiation, and pollution. Furthermore, the monitoring is used to react to the threats caused by the natural hazards as well as follow the effects of the international protocols.

Therefore, monitoring the chemical composition and radiation of the atmosphere is a very important duty for EUMETSAT and the target is to provide information for policy makers, scientists and general public.

Objectives

The main objectives of the AC SAF is to process, archive, validate and disseminate atmospheric composition products (O_3, NO_2, SO_2, BrO, HCHO, H_2O, OClO, CO, NH3), aerosol products and surface ultraviolet radiation products utilising the satellites of EUMETSAT. The majority of the AC SAF products are based on data from the GOME-2 and IASI instruments onboard Metop satellites.

Another important task besides the near real-time (NRT) and offline data dissemination is the provision of long-term, high-quality atmospheric composition products resulting from reprocessing activities.

Product categories, timeliness and dissemination

NRT products are available in less than three hours after measurement. These products are disseminated via EUMETCast, WMO GTS or internet.

- Near real-time trace gas columns (total and tropospheric O_3 and NO_2, total SO_2, total HCHO, CO) and high-resolution ozone profiles
- Near real-time absorbing aerosol indexes from main science channels and polarization measurement detectors
- Near real-time UV indexes, clear-sky and cloud-corrected

Offline products are available within two weeks after measurement and disseminated via dedicated web services at EUMETSAT and AC SAF.

- Offline trace gas columns (total and tropospheric O_3 and NO_2, total SO_2, total BrO, total HCHO, total H_2O) and high-resolution ozone profiles
- Offline absorbing aerosol indexes from main science channels and polarization measurement detectors
- Offline surface UV, daily doses and daily maximum values with several weighting functions

Data records are available after reprocessing activities from the EUMETSAT Data Centre and/or the AC SAF archives.

- Data records generated in reprocessing
- Lambertian-equivalent reflectivity
- Total OClO

Users can access the AC SAF offline products and data records (free of charge) by registering at the AC SAF web site.

More information about the AC SAF project, products and services: https://acsaf.org/
AC SAF Helpdesk: helpdesk@acsaf.org
Twitter: https://twitter.com/Atmospheric_SAF

ACRONYMS AND ABBREVIATIONS

AUTH	Aristotle University of Thessaloniki
BIRA	Royal Belgian Institute for Space Aeronomie
BUFR	Binary Universal Form for the Representation of meteorological data
CDOP	Continues Development and Operations Proposal
EUMETSAT	European Organisation for the Exploitation of Meteorological Satellites
MetOp	Meteorological Operational satellite
NRT	Near-real-time
SO_2	Sulphur dioxide

Applicable AC SAF Documents

[ATBD] **IASI Brescia SO_2 Algorithm Theoretical Basis Document**, SAF/O3M/ULB/BresciaSO2_ATBD, Issue 1.1, 28/07/2016, L. Clarisse, D. Hurtmans , P.-F. Coheur, R. Astoreca, M.George and C. Clerbaux, https://acsaf.org/docs/atbd/Algorithm_Theoretical_Basis_Document_IASI_SO2_Jul_2016.pdf, last accessed: 08.04.2021

[PUM] **Product User Manual for the Near real-time IASI Brescia SO_2,** SAF/AC/ULB/PUM/002, issue 1.2, 28.03.2018, R. Astoreca, D. Hurtmans, L Clarisse, P. Coheur, M. George, J. Hadji-Lazaro and C. Clerbaux, https://acsaf.org/docs/pum/Product_User_Manual_IASI_SO2_Mar_2018.pdf, last accessed: 08.04.2021

[PRD] **AC SAF Product Requirements Document**, SAF/AC/FMI/RQ/PRD/001, Issue 1.7, J. Hovila, S. Hassinen, P. Valks, S. Kiemle, O. Tuinder and H. Joench-Soerensen, 01.09.2020 [internal ACSAF document]

[VR] **AC SAF IASI/MetopA & IASI/MetopB Sulphur Dioxide Validation Report,** SAF/O3M/AUTH/ORR/SO2/IASI, 17.11.2017, Koukouli, M., G.Pinardi, M. George, N. Theys, L. Clarisse and R. Astoreca, https://acsaf.org/docs/vr/Validation_Report_IASI_SO2_Nov_2017.pdf, last accessed: 07.04.2021.

References

Clarisse, L., Hurtmans, D., Clerbaux, C., Hadji-Lazaro, J., Ngadi, Y. and Coheur, P. F.: Retrieval of sulphur dioxide from the infrared atmospheric sounding interferometer (IASI), Atmos. Meas. Tech., 5, 581-594, doi:10.5194/amt-5-581-2012, 2012.

Technical information

Satellite ID: M03
Product type: O3M-57, O3M-377 | MxI-N-SO2
Validation reporting period **September 2019 – March 2021**
Level-2 processor version Brescia v6.05

Input IASI/MetOp-C Level-1B data version table

Start Date	*Start Orbit*	*Level 1B Version*
September 20, 2019	4507	7.4

Acknowledgments

Part of the results presented in this work have been produced using the Aristotle University of Thessaloniki High Performance Computing Infrastructure and Resources. M.K. would like to acknowledge the support provided by the IT Center of the Aristotle University of Thessaloniki throughout the progress of this research work. M.K. further acknowledges the support by the Atmospheric Toolbox®.

Table of contents

Table of Figures

1 INTRODUCTION

Scope of this document

The present document reports on the validation of the NRT IASI/MetOp-C, here-after IASI-C, sulphur dioxide, SO_2, columns, between September 2019 and March 2021. The data are produced operationally by the Brescia version 6.05 operated at EUMETSAT and are distributed via EumetCAST in BUFR format. This report addresses the quality, stability and continuity of the IASI-C dataset, compared to its sister instruments of IASI/MetopA [IASI-A] and IASI/Metop-B [IASI-B]. As the three instruments are known to be of equal quality and not to suffer from degradation effects, this report inter-compares the IASI-C columns to those of the other two sensors. The two former instruments were extensively validated against other satellite products as well as ground-based observations, for a number of volcanic eruptions and anthropogenic SO_2 cases already in the [VR]. It hence follows that by directly comparing the newer instruments, IASI-C, to the former ones, we can indirectly validate this sensor as well.

IASI/Metop SO_2 Product requirements

In the following we reproduce the table that pertains to the total sulphur dioxide IASI/Metop products where the accuracy requirements are given as 200% [threshold], 100% [target] and 50% as the optimal accuracy for columns assumed to be below 10km, while above 10km those requirements are reduced to 100%, 35% and 20% respectively.

Table 1.1. The relevant table from the Product Requirements Document [PRD].

NRT IASI SO2		
O3M-57, O3M-377	**MxI-N-SO2**	
Type	Product	
Applications and users	Climate studies, volcanic monitoring (VAACs)	
Characteristics and methods	LUT	
Generation frequency	PDU dissemination frequency, every 3 minutes	
Input satellite data	Metop-A/B/C: IASI	
Algorithm version	v20150205_sp20171122	
Dissemination		
Type	Format	Means
NRT	BUFR, HDF5	EUMETCast, WMO GTS
Accuracy below 10 km		
Threshold	Target	Optimal
200 %	100 %	50 %
Accuracy above 10 km		
Threshold	Target	Optimal
100 %	35 %	20 %
Verification method	Other satellite data and possibly ground-based measurements	
Coverage, resolution and timeliness		
Spatial coverage	Spatial resolution	Timeliness

Global	IASI spatial resolution, cloud fraction below 20 %	≤ 3 hours
Comments		
Accuracies are highly dependent on the altitude of the SO_2 plume. The percentages in this table assume knowledge of the altitude, temperature and pressure of the SO_2 layer, and in addition assume no major cloud and aerosol contamination. The operational range of the algorithm is 0.5-5000 DU (depending on the altitude).		

Summary of the findings of the Validation Report [VR] of IASI-A and IASI-B SO_2 columns

The VR investigated the quality of the IASI/MetopA (2007-2013) and IASI/MetopB (June – October 2017) Brescia v201510 SO_2 columns by comparing them to ground-based measurements performed on a global scale by Brewer and MAXDOAS spectrophotometers, as well as satellite observations obtained by the OMI/Aura and GOME2/MetopA instruments. Different spatiotemporal collocation criteria were applied depending on the comparisons as well as different restriction criteria. The report is focused solely on SO_2 of volcanic provenance, and mainly from eruptive events at that.

The following main conclusions were drawn:

- Eleven major eruptive events were analysed in detail vis-a-vis the loadings observed by IASI/MetopA & /MetopB in comparison to OMI/Aura and GOME2/MetopA. Different assumptions in plume heights within the equivalent algorithms were all considered. The analysis on SO_2 masses showed that, for the entire eruption episodes, the correlations range between 0.70 and 0.95 depending on the plume height and satellite instrument. The IASI 13 & 16km plumes showed the best agreement to the OMI/Aura 15km plume mostly around ±20%.
- The results were within the user requirements as stated in the Product Requirements Document [Table 1.1] namely, below 10 km, the target accuracy of 100 % was found to be achieved whereas above 10km the optimal accuracy of 50% was achieved for the EUMETSAT NRT_PPF_v6.3 IASI products.

Roadmap of this document

A short overview of the IASI/Metop datasets presented in this work is given in the Data and Methodology, in subsection 2.1, while the case studies used as validation tools are briefly discussed in subsection 2.2. The results of this validation study are presented in four subsections of the main results Section 3, for each of the four volcanic eruptions identified during the timeline of this report. Due to the very different natures of the volcanic eruptions these cannot be assumed as one comparative dataset. Since the main premise of this validation is to show that IASI-C senses the same atmospheric state as the two previously established sensors, IASI-A & IASI-B, the findings are always provided separately for those two sensors. Summary and recommendations follow in the Conclusions Section 4.

2 DATA AND METHODOLOGY

2.1 IASI/MetoP EUMETSAT NRT data

The IASI datasets presented in this report are distributed by EUMETSAT via EumetCAST in BUFR format. The IASI Level 2 SO2 BUFR PDU file structure and descriptors are given in Appendix A, as extracted from the PUM. The Brescia algorithm calculates IASI SO2 total columns using brightness temperature differences and look up tables assuming 5 different plumes heights (7, 10, 13, 16 and 25 km). The algorithm description is given in the Brescia ATBD [ATBD] and in Clarisse et al., 2012. When the IASI L2 pressure and temperature profiles are not available, ECMWF forecasts (3h, interpolated in time and space) data are used. A flag is provided in order for the user to separate these cases whereupon the flag takes the value of 9, SO2_QFAG=9 (default value), the value of 11, SO2_QFAG=11. The SO2_QFLAG contained an anomaly (see announcement 5295 of EUMETSAT user notification service) for part of the timeline shown in this report and is therefore not used (confirmed after personal communication with EUMETSAT). As an alternative, in the following work, we used the commonly accepted Brightness Temperature, BT, Difference (SO2_BT_DIFFERENCE) as indicator for a volcanic plume. The recommendation in the PUM is that only retrievals in the neighborhood of pixels with SO2_BT_DIFFERENCE>1K pixels, and pixels with a SO2_BT_DIFFERENCE < 0.4 K should definitely not be used as thiscut-off signifies that not enough signal is available for a dependable SO_2 retrieval.

2.2 Volcanic eruptions

During the time period between September 2019 and March 2021, four significant eruptions were identified; the Taal, Philippines, eruption in January 2020 (**Figure 1**); the Anak Krakatau, Indonesia, eruption in April 2020 (**Figure 2**); the Nishinoshima, Japan, eruption in July 2020 (**Figure 3**) and the recent eruptions by Mt. Etna, Italy, in February & March 2021 (**Figure 4**). For each of these eruptive periods, the IASI SO_2 columns reported for the heights of 7, 10, 13 and 16 km are compared in the results section.

Taal Philippines | 12 January 2020

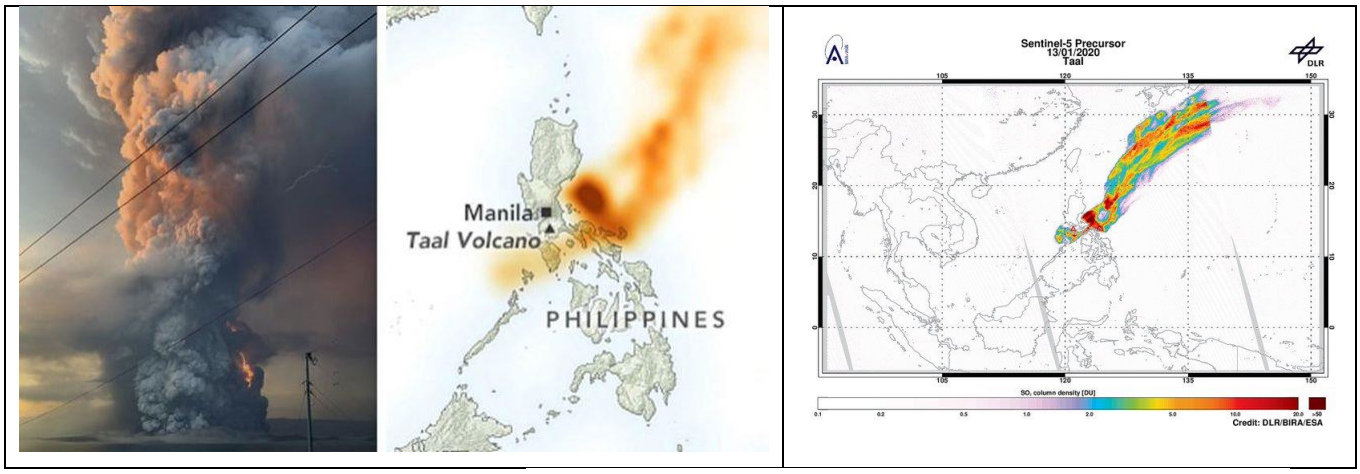

Figure 1. Left. Taal eruptive plume and stratospheric sulfur dioxide concentrations on January 13, 2020, as detected by the Ozone Mapping Profiler Suite (OMPS) on the NOAA-NASA Suomi-NPP instrument. Right. Same day sulfur dioxide observations by the S5P/TROPOMI instrument. Source: https://twitter.com/DlrSo2

Anak Krakatau | April 2020

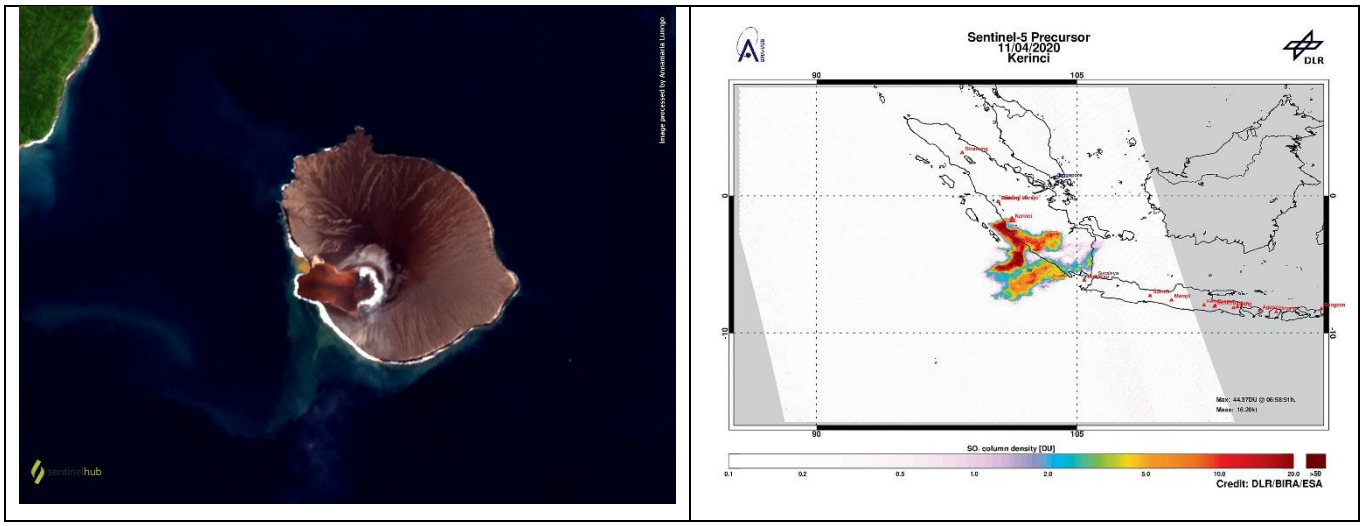

Figure 2. Left. The Anak Krakatau caldera, after the eruption of April 2020. Right. The SO_2 load observed by the S5P/TROPOMI instrument for April 11th, 2020. Source: https://twitter.com/DlrSo2

Nishinoshima, Japan | July-August 2020

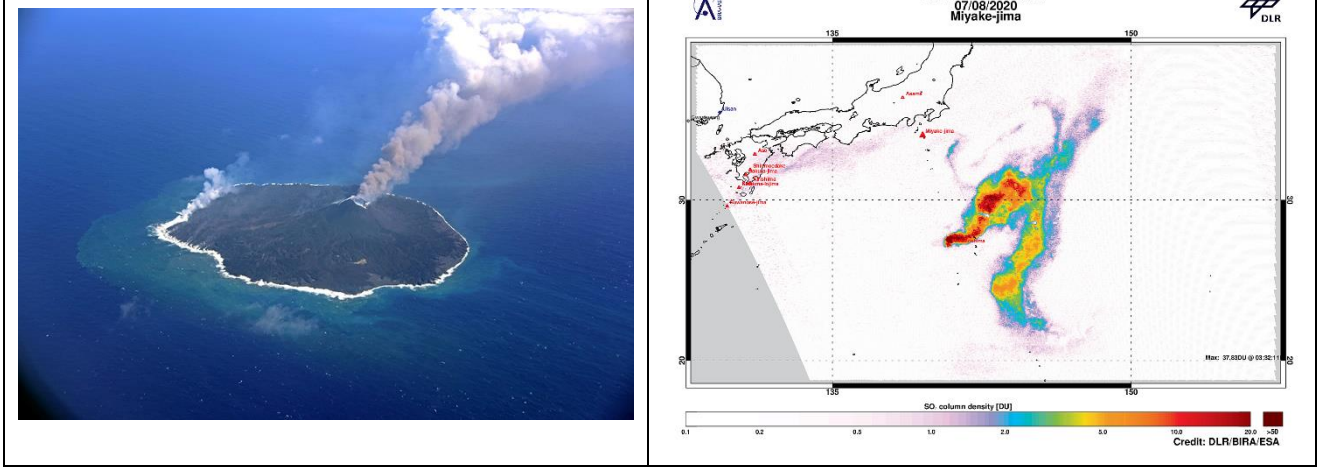

Figure 3. Left. Outgassing by the Nishinoshima volcano. Right. The SO_2 load observed by the S5P/TROPOMI instrument for August 7th, 2020. Source: https://twitter.com/DlrSo2

Mt Etna, Italy | February – April 2021

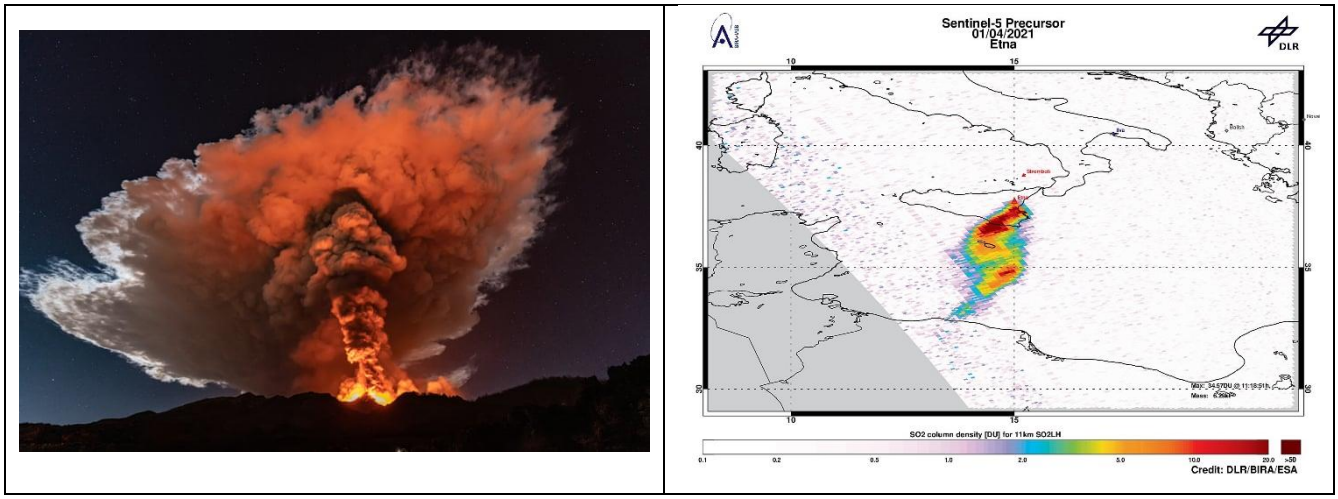

Figure 4. Right. The eruptive cloud of Mt Etna, Italy. Right. The SO_2 load observed by the S5P/TROPOMI instrument for April 1st, 2021. Source: https://twitter.com/DlrSo2

3 RESULTS

In the following section, the comparisons between the four different reported SO_2 columns for the four different assumed plume heights is shown between IASI-C and, separately, IASI-A and IASI-B. The Taal eruption is extensively discussed, demonstrating the validation chain process, while for the other three eruptions the major findings and statistics will be presented. Tables of statistics are included at the end of each sub-section.

3.1 Taal, Philippines | 20200113 to 20200119

Daily gridded datasets, at 0.2x0.2°, were created for all sensors for the timeline of the Taal 2020 eruption, between the 13th and the 19th of January 2020. Both day- and night-time, which are 12h later, observations, were first taken into account, with a BT difference filter of > 0.4K. An example is shown in **Figure 5** where the 14th of January 2020 is shown for the IASI-A [upper], IASI-B [middle] and IASI-C [lower] sensors. The multi-plots show the four reported SO_2 columns for 16 km [upper left], for 13 km [upper right], for 10 km [bottom left] and for 7 km [bottom right.] All sensors report the location of the plume, with any differences seen being attributed to the slightly different overpass times of the Metop platforms. In order to separate this effect, the observations were separated into AM and PM, and daily gridded datasets, at 0.2x0.2°, were further created.

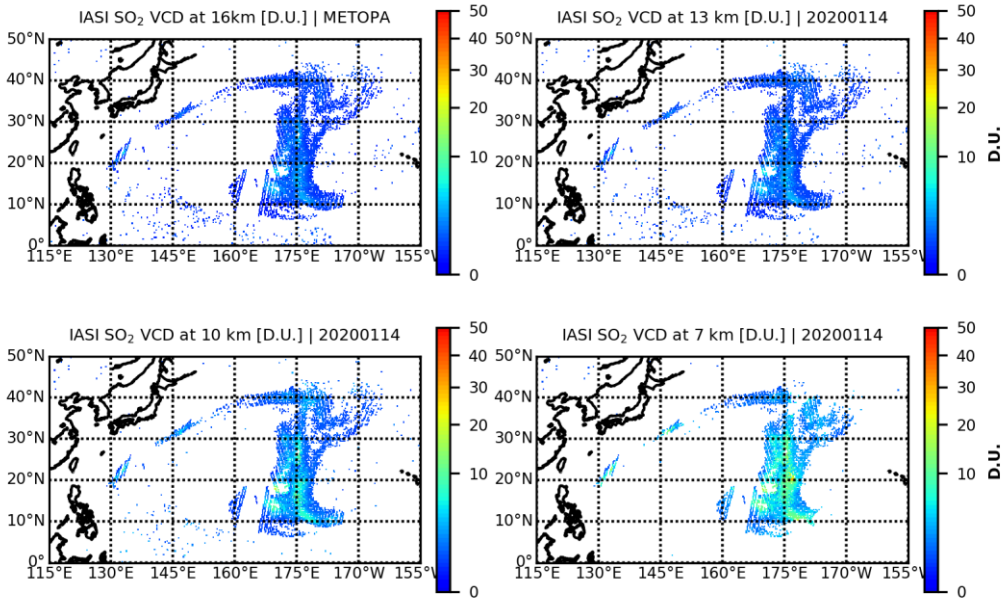

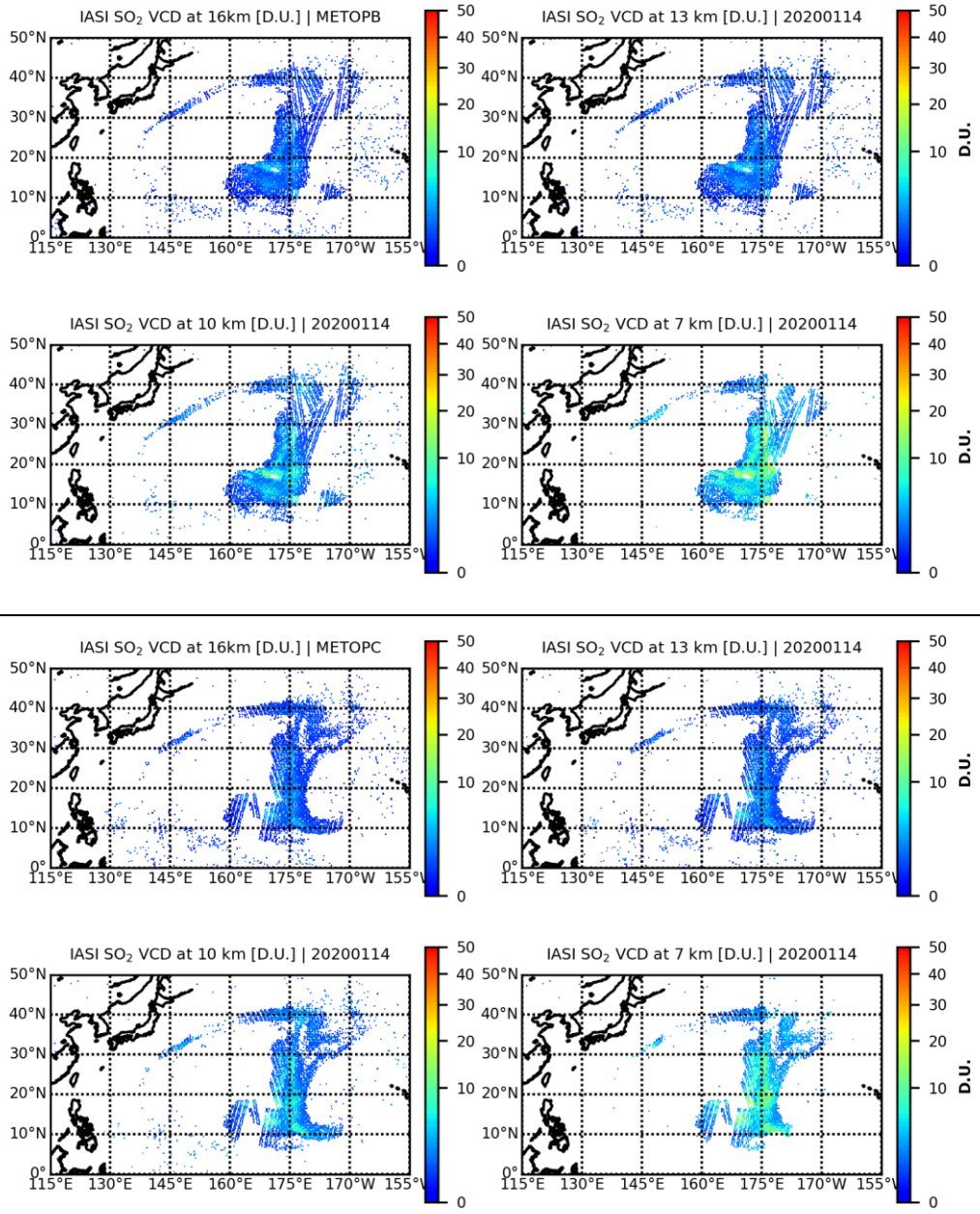

Figure 5. Example of the daily mean coverage of IASI-A [upper], IASI-B [middle] and IASI-C [lower] for the Taal eruption on the 14th of January 2020. The multi-plots show the four reported SO_2 columns for 16 km [upper left], for 13 km [upper right], for 10 km [bottom left] and for 7 km [bottom right.] Gridded at 0.2x0.2°.

In **Figure 6**, the mean coverage of the daylight [AM] hours for IASI-A [upper], IASI-B [middle] and IASI-C [lower] for the Taal eruption on the 14th of January 2020, as per**Figure 5**. Different patterns can already be identified between IASI-A & IASI-C compared to IASI-B, which are not as prominent for the night-time [PM] hours, shown in **Figure 7**.

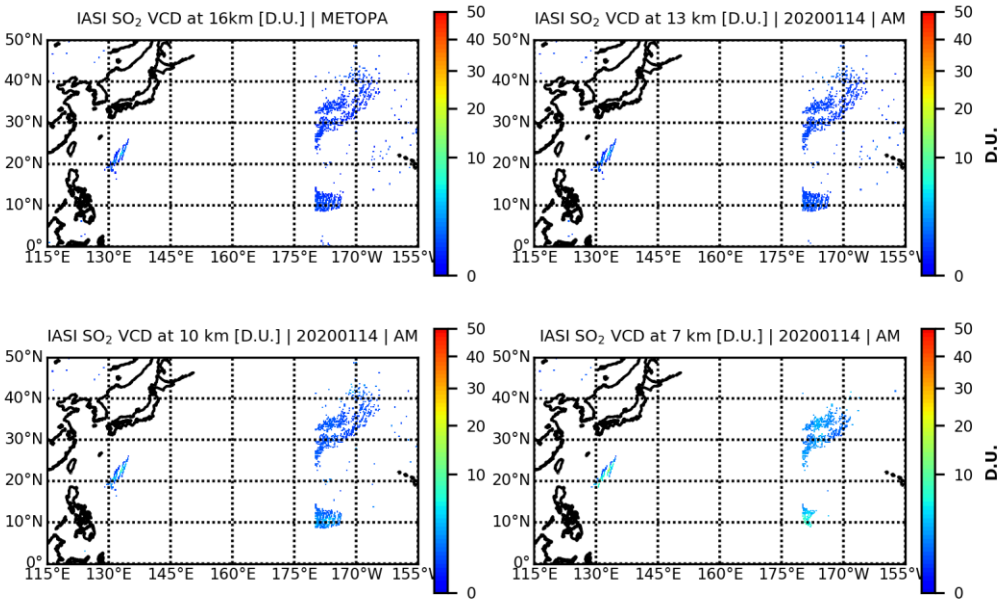
IASI SO2 VCD at 16km [D.U.] | METOPA
IASI SO2 VCD at 13 km [D.U.] | 20200114 | AM
IASI SO2 VCD at 10 km [D.U.] | 20200114 | AM
IASI SO2 VCD at 7 km [D.U.] | 20200114 | AM
50°N
40°N
30°N
20°N
10°N
0°
115°E 130°E 145°E 160°E 175°E 170°W 155°W
50
40
30
20
10
0
D.U.

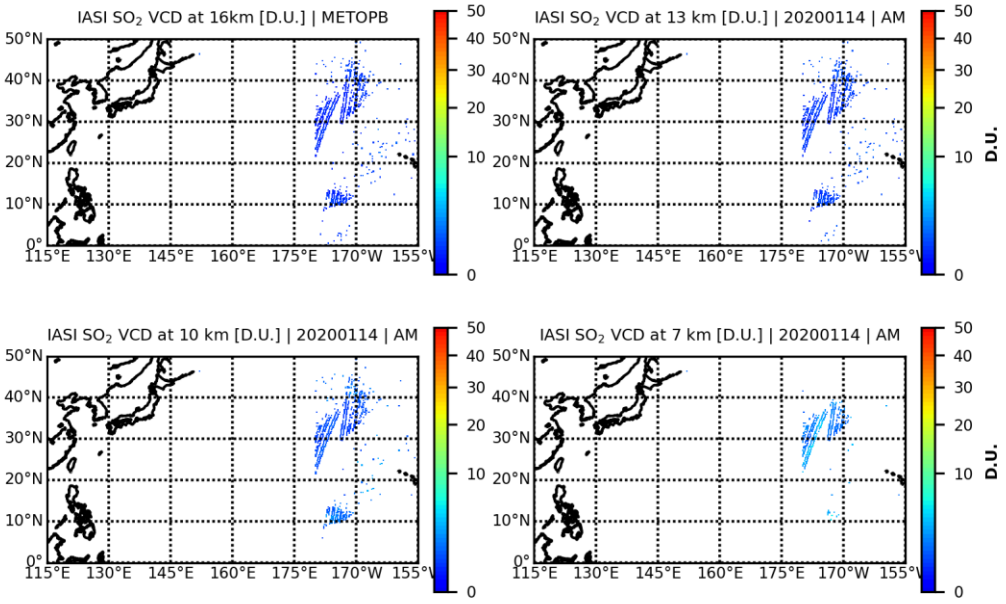
IASI SO2 VCD at 16km [D.U.] | METOPB
IASI SO2 VCD at 13 km [D.U.] | 20200114 | AM
IASI SO2 VCD at 10 km [D.U.] | 20200114 | AM
IASI SO2 VCD at 7 km [D.U.] | 20200114 | AM
50°N
40°N
30°N
20°N
10°N
0°
115°E 130°E 145°E 160°E 175°E 170°W 155°W
50
40
30
20
10
0
D.U.

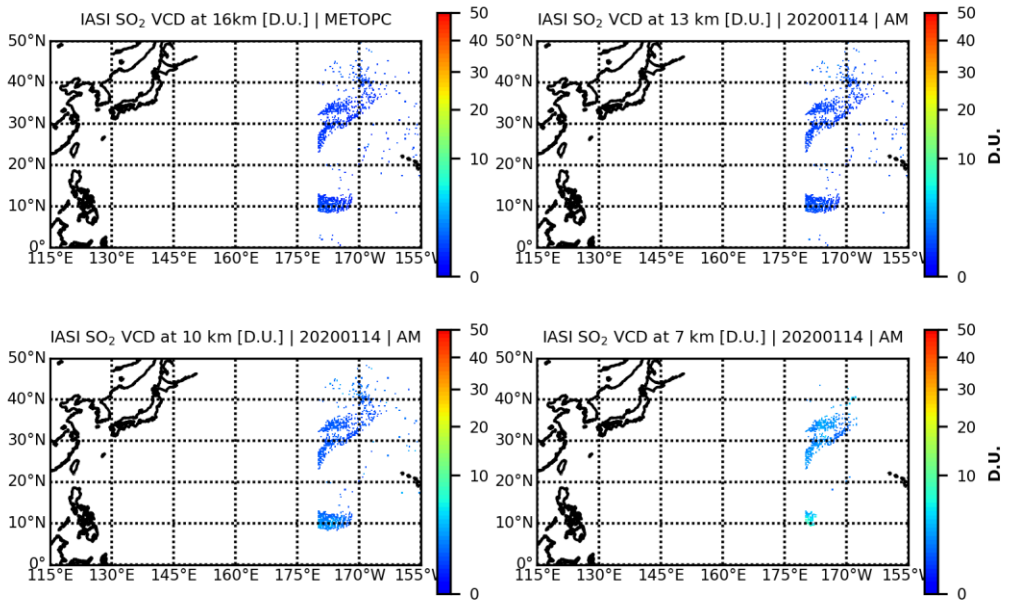

Figure 6. Example of the mean coverage for the local AM hours of IASI-A [upper], IASI-B [middle] and IASI-C [lower] for the Taal eruption on the 14th of January 2020. The multi-plots show the four reported SO_2 columns for 16 km [upper left], for 13 km [upper right], for 10 km [bottom left] and for 7 km [bottom right.] Gridded at 0.2x0.2°.

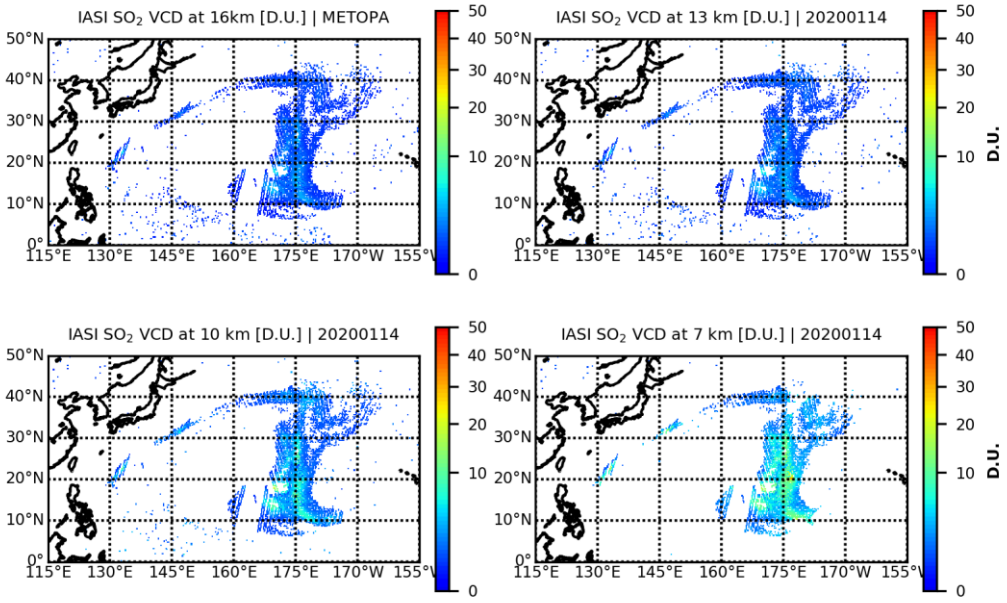

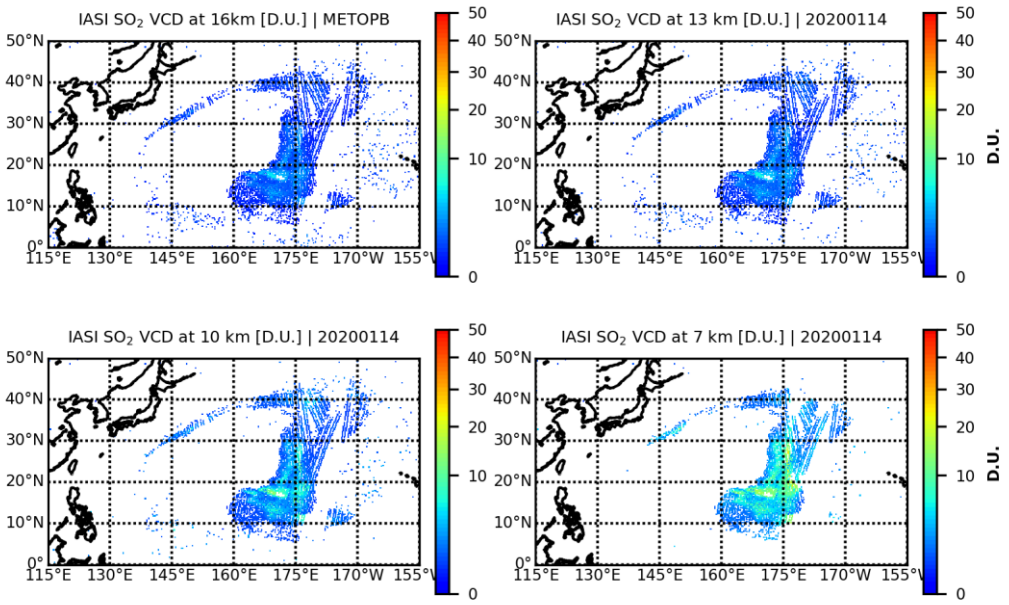

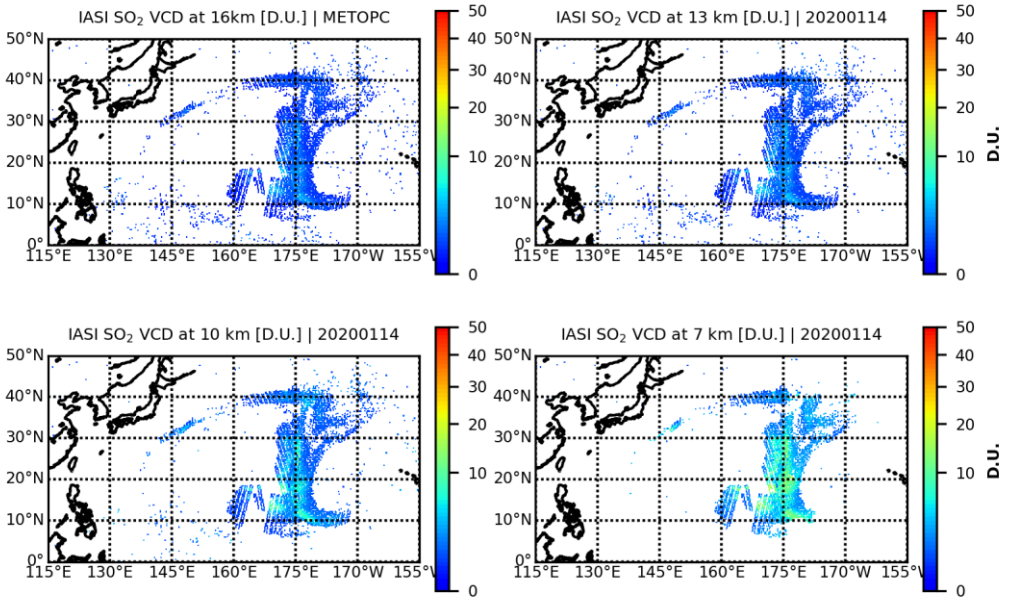

Figure 7. As per **Figure 6**, but for the PM local times.

The datasets were then gridded onto the same 0.2x0.2°, for eight 3h intervals during each sensing day. Scatter plots for all four assumed plume heights are shown in **Figure 8**, including the correlation coefficient and linear fit. Comparisons to IASI-A [upper] show excellent agreement with slopes between 0.9 and 1 and correlations between 0.902 and 0.932. Slightly decreased correlations are shown for IASI-B [lower] however still excellent, between 0.842 and 0.865, with slopes between 0.8 and 0.9.

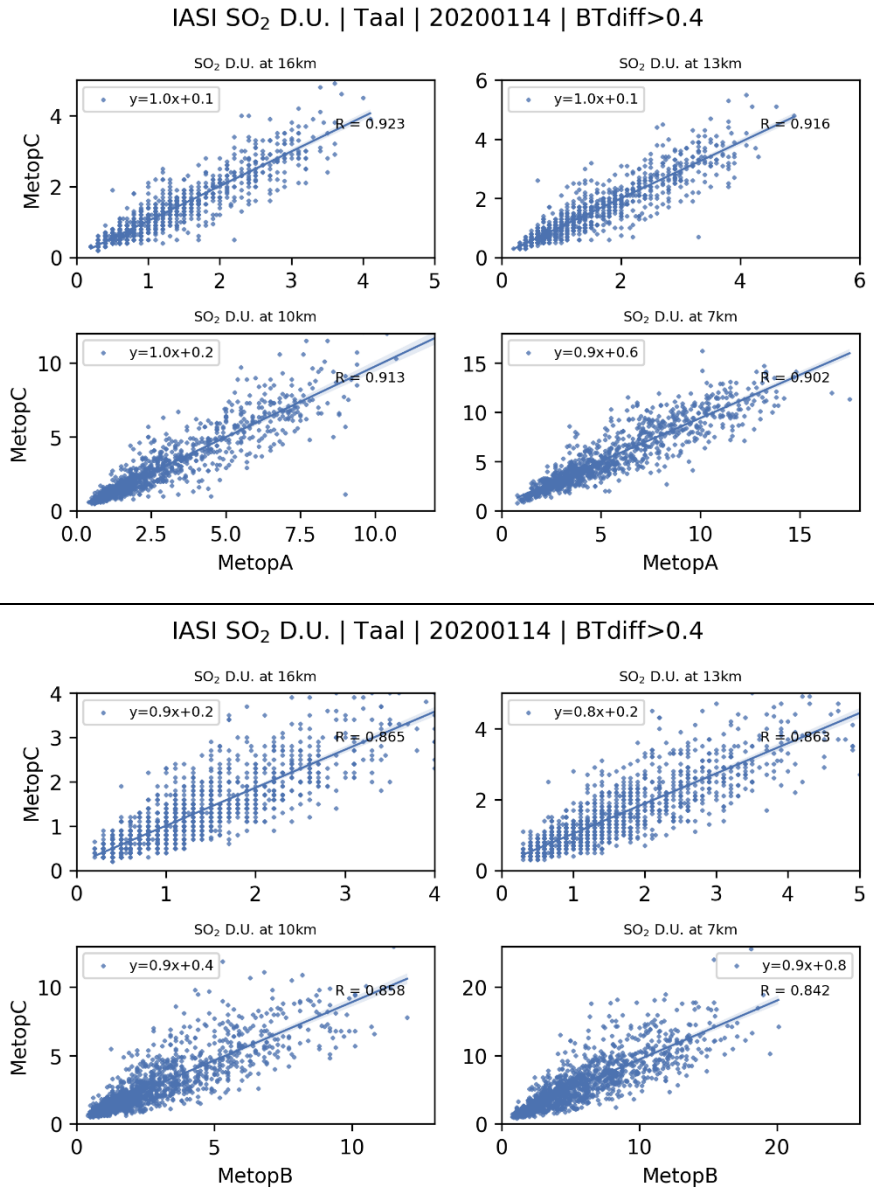

Figure 8. Scatter plots for the 3h common geographical points between IASI-C and IASI-A [upper] and IASI-B [lower] the Taal eruption on the 14th of January 2020. The multi-plots show the four reported SO_2 columns for 16 km [upper left], for 13 km [upper right], for 10 km [bottom left] and for 7 km [bottom right.] Gridded at 0.2x0.2°.

The differences are also shown as a histogram representation, in bins of 2 D.U., in **Figure 9**, where the comparisons to IASI-A are shown at the top and to IASI-B at the bottom. The mean difference, standard deviation and number of common points are also insert. For the comparisons to IASI-A the mean difference for the 14th of January 2020 is basically 0 D.U. and the standard deviations range from the lowest 0.33D.U. for the higher-most column, at 16km, to 1.36D.U. for the lowermost column, at 7km. Similarly for IASI-B, near zero differences and standard deviations between 0.40 and 2 D.U. for the lowermost reported column.

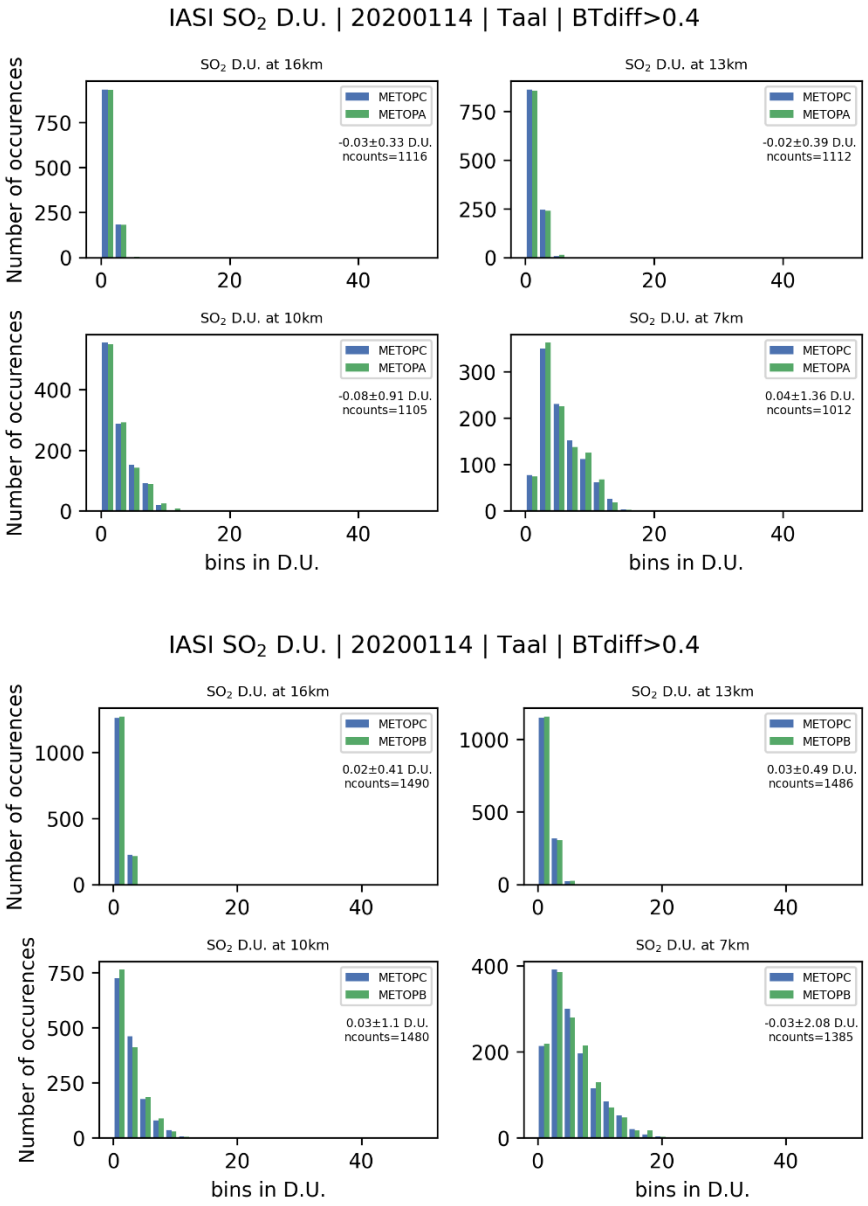

Figure 9. Histogram plots for the 3h common geographical points between IASI-C and IASI-A [upper] and IASI-B [lower] the Taal eruption on the 14th of January 2020. The multi-plots show the four reported SO_2 columns for 16 km [upper left], for 13 km [upper right], for 10 km [bottom left] and for 7 km [bottom right.] Gridded at 0.2x0.2°.

Moving on to the entire volcanic eruption of Taal, between January 13 and January 19th, the scatter plot for the 3h common geographical points between IASI-C and IASI-A [upper] and IASI-B [lower] is shown in **Figure 10**. Comparisons to IASI-A [upper] show slopes between 0.8 and 0.9 and correlations between 0.770 and 0.837. Slightly decreased correlations are shown for IASI-B [lower], between 0.785 and 0.795, with slopes between 0.7 and 0.8.

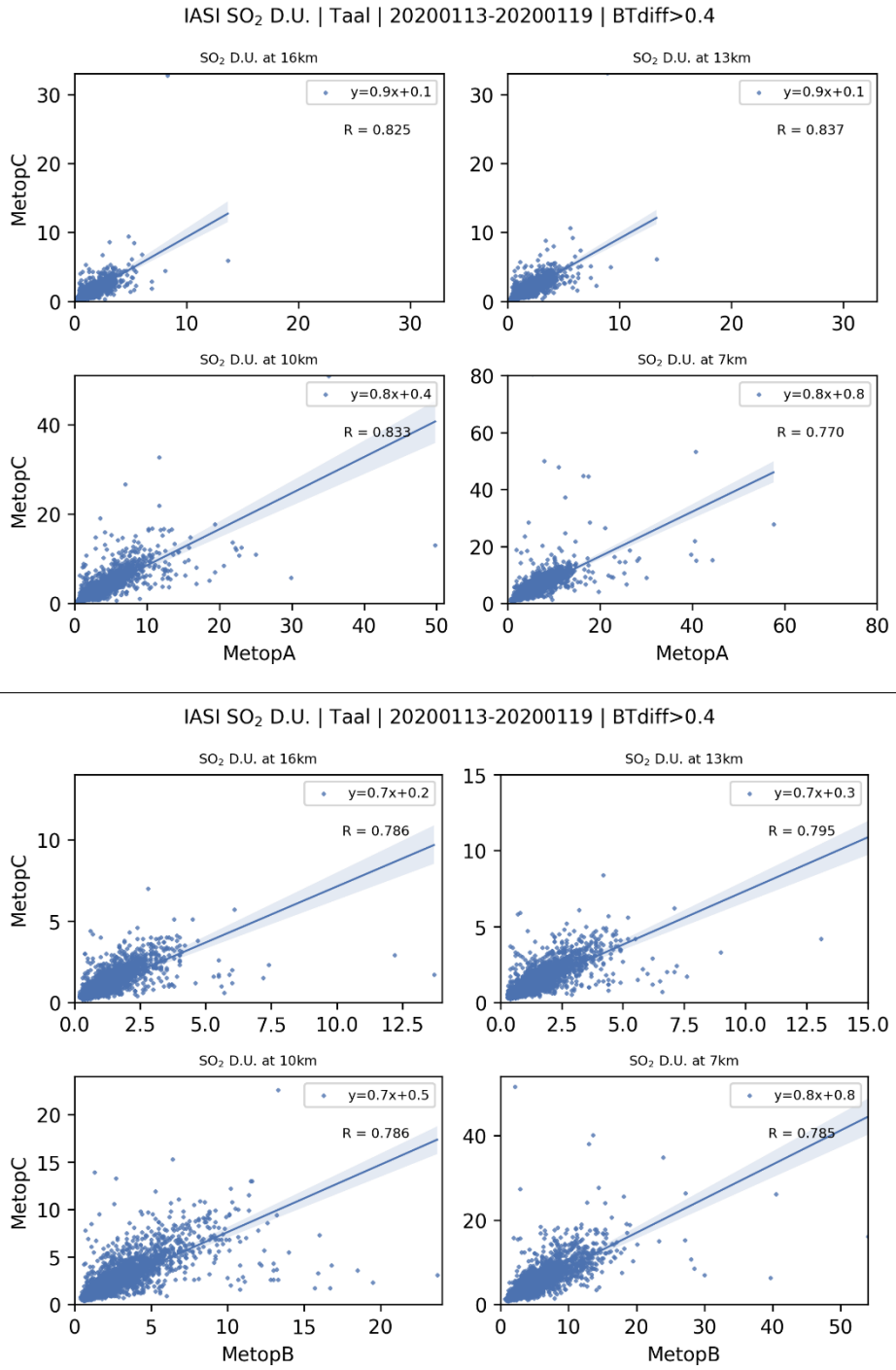

Figure 10. Scatter plots for the 3h common geographical points between IASI-C and IASI-A [upper] and IASI-B [lower] the entire Taal eruption, 13 to 19th of January 2020. The multi-plots show the four reported SO_2 columns for 16 km [upper left], for 13 km [upper right], for 10 km [bottom left] and for 7 km [bottom right.] Gridded at 0.2x0.2°.

Overall, the statistics remain excellent (**Figure 11**) with mean differences around 0 D.U. and std between 0.4 and 2 D.U. for both sensors for the entire Taal eruption, 13 to 19th of January 2020.

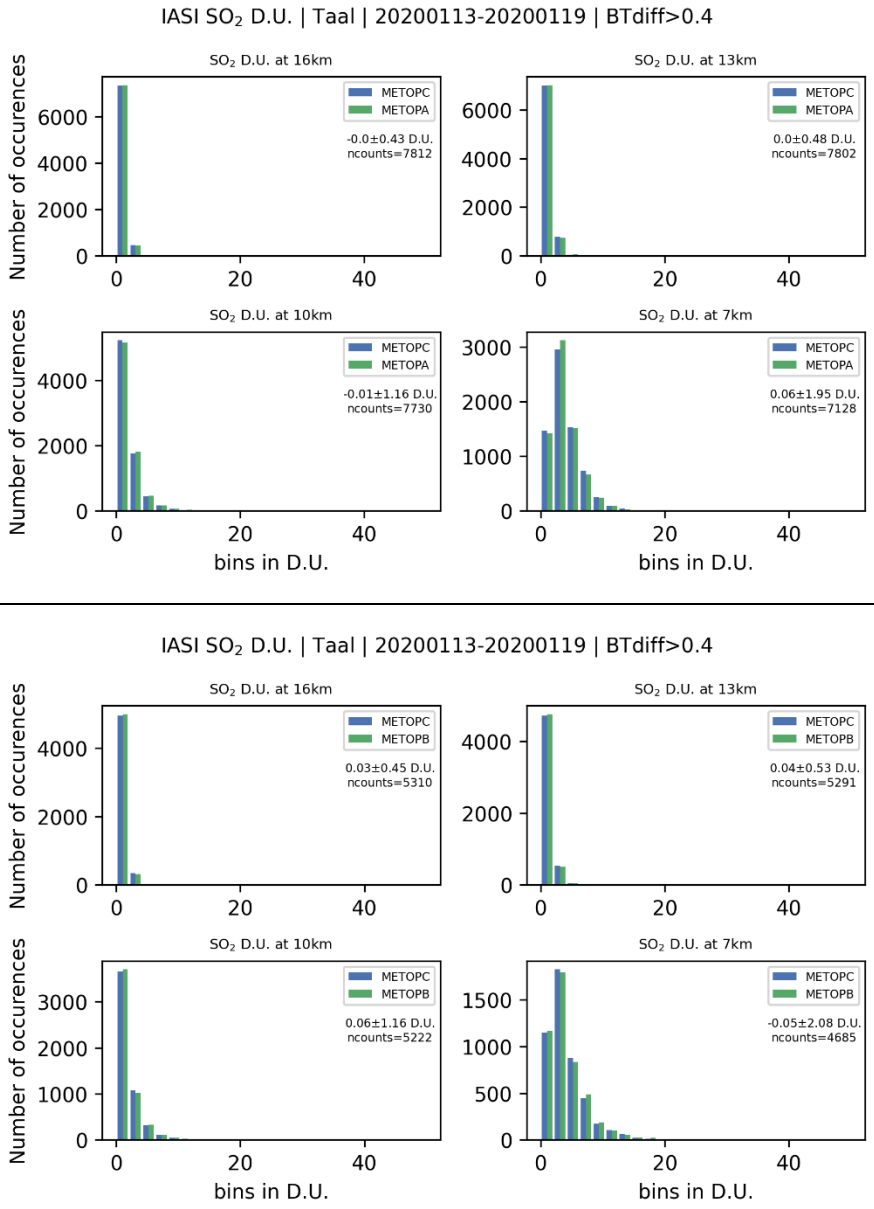

Figure 11. Histogram plots for the 3h common geographical points between IASI-C and IASI-A [upper] and IASI-B [lower] the entire Taal eruption, 13 to 19th of January 2020. The multi-plots show the four reported SO_2 columns for 16 km [upper left], for 13 km [upper right], for 10 km [bottom left] and for 7 km [bottom right.] Gridded at 0.2x0.2°.

Table 3.2 Mean difference, standard deviation and number of collocations for the Taal eruption, 13 to 19th of January 2020.

IASI/MetopC	**vs IASI/MetopA**		**vs IASI/MetopB**	
Plume height	mean ± std	counts	mean ± std	counts
16km	-0.0 ± 0.43 D.U.	7812	0.03 ± 0.45 D.U.	5310
13km	0.0 ± 0.48 D.U.	7802	0.04 ± 0.53 D.U.	5291

10km	-0.01 ± 1.16 D.U.	7730	0.06 ± 1.16 D.U.	5222
7km	0.06 ± 1.95 D.U.	7128	-0.05 ± 2.08 D.U.	4685

Table 3.3. Slope, intercept and correlation coefficient for the Taal eruption, 13 to 19th of January 2020, collocations.

IASI/MetopC	**vs IASI/MetopA**			**vs IASI/MetopB**		
Plume height	Slope	Intercept	R value	Slope	Intercept	R value
16km	0.923	0.075	0.825	0.689	0.241	0.786
13km	0.901	0.106	0.837	0.706	0.277	0.795
10km	0.810	0.410	0.833	0.711	0.512	0.786
7km	0.785	0.816	0.770	0.808	0.846	0.785

Even though the three datasets are in agreement, the differences between comparing to IASI-A and IASI-B could only be explained by the slightly different sensing time of the instruments, and the rapid spatial variability of the wind-driven volcanic plumes. An example of the temporal differences between sensing time of IASI-C and IASI-B are shown in **Figure** 22 (Appendix B) where it is shown that, even though the larger part of the orbits are within ±60min, there exists locations where this rises significantly. As a result, we repeated the above comparisons, gridding onto the same 0.2x0.2°, but for twenty-four 1h intervals during each sensing day.

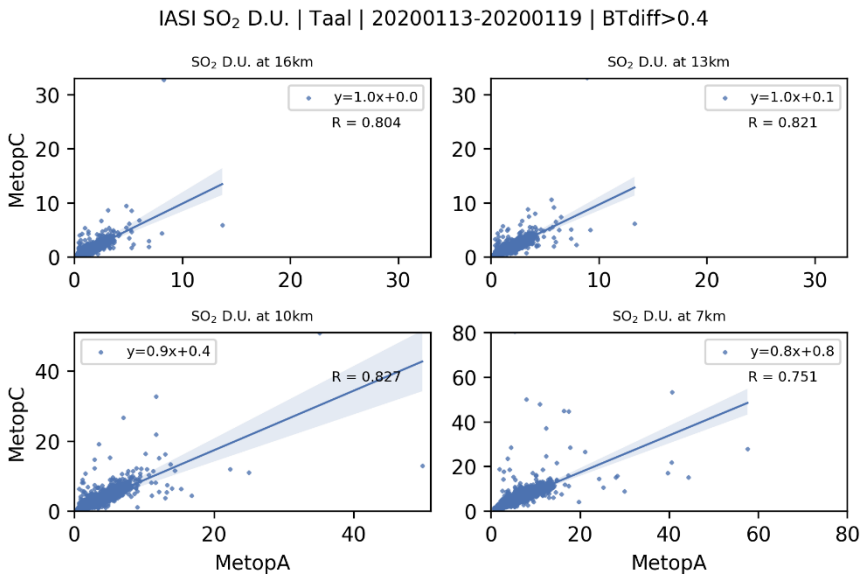

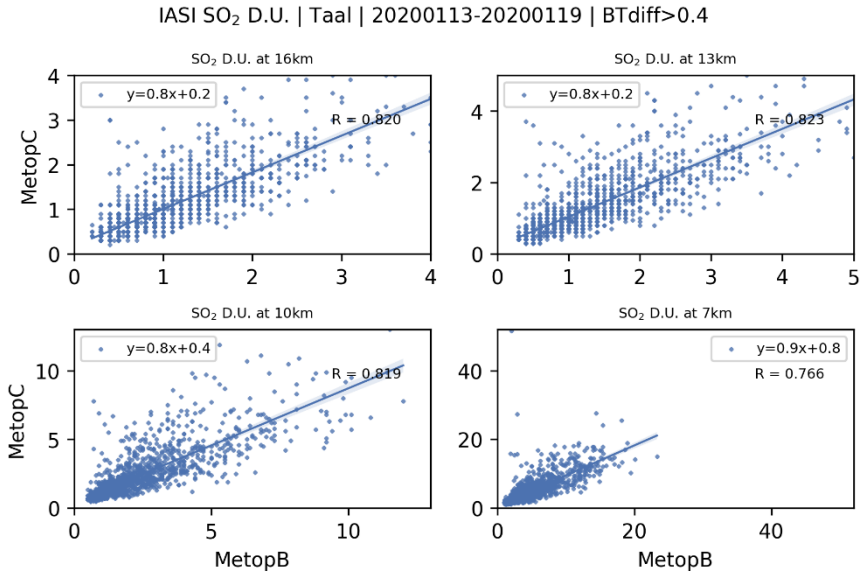

Figure 12. Scatter plots for the 1h common geographical points between IASI-C and IASI-A [upper] and IASI-B [lower] the entire Taal eruption, 13 to 19th of January 2020. The multi-plots show the four reported SO_2 columns for 16 km [upper left], for 13 km [upper right], for 10 km [bottom left] and for 7 km [bottom right.] Gridded at 0.2x0.2°.

Table 3.4. Slope, intercept and correlation coefficient for the Taal eruption, 13 to 19th of January 2020, collocations, for the 1h sampling grids.

IASI/MetopC	**vs IASI/MetopA**			**vs IASI/MetopB**		
Plume height	Slope	Intercept	R value	Slope	Intercept	R value
16km	0.978	0.044	0.804	0.822	0.182	0.820
13km	0.958	0.067	0.821	0.821	0.216	0.823
10km	0.851	0.356	0.827	0.832	0.397	0.819
7km	0.828	0.758	0.751	0.873	0.773	0.766

The marked improvement for the comparisons between IASI-C and IASI-B points to the fact that a strict temporal criterion is paramount when inter-comparing the two, or when merging the dataset to create a uniform dataset based on IASI SO_2 columns.

3.2 Anak Krakatau, Indonesia | 20200411 to 20200413

For the case of the eruption of Anak Krakatau, Indonesia, in April 2020, three eruptive days are shown in the following comparisons. In this case, however, choosing a temporal criterion of 1h was found to produce very few spatial collocations between IASI-C and IASI-B. We hence present in the following comparisons based on a temporal collocation of 3h fields, while keeping in mind the rapidly varying Krakatau plumes. As above, we fist give an example for this eruption. In **Figure 13**, the daily mean coverage of IASI-A [upper], IASI-B [middle] and IASI-C [lower] for the Anak Krakatau eruption on the 12th of April 2020 are shown. The multi-plots show the four reported SO_2 columns for 16 km [upper left], for 13 km [upper right], for 10 km [bottom left] and for 7 km [bottom right] gridded at 0.2x0.2°.

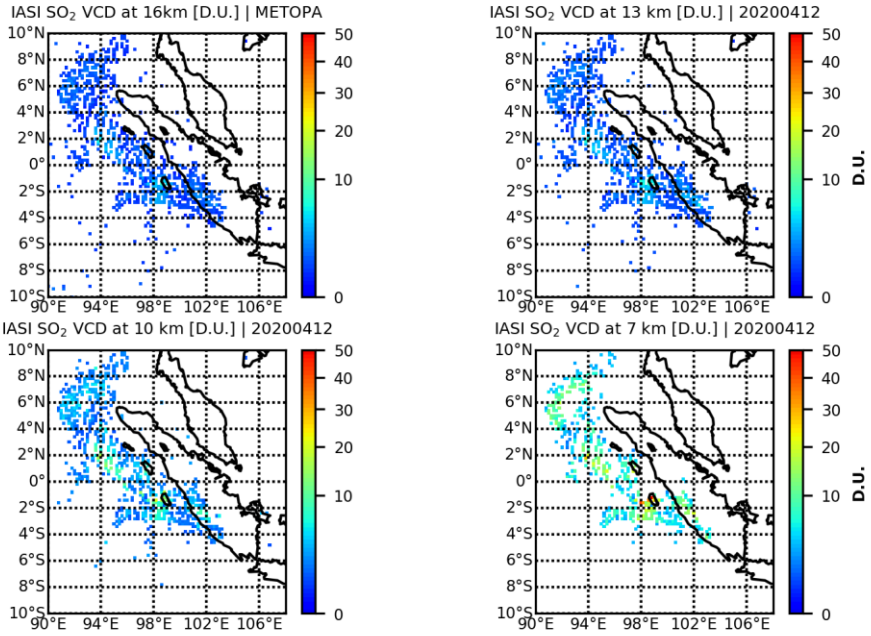

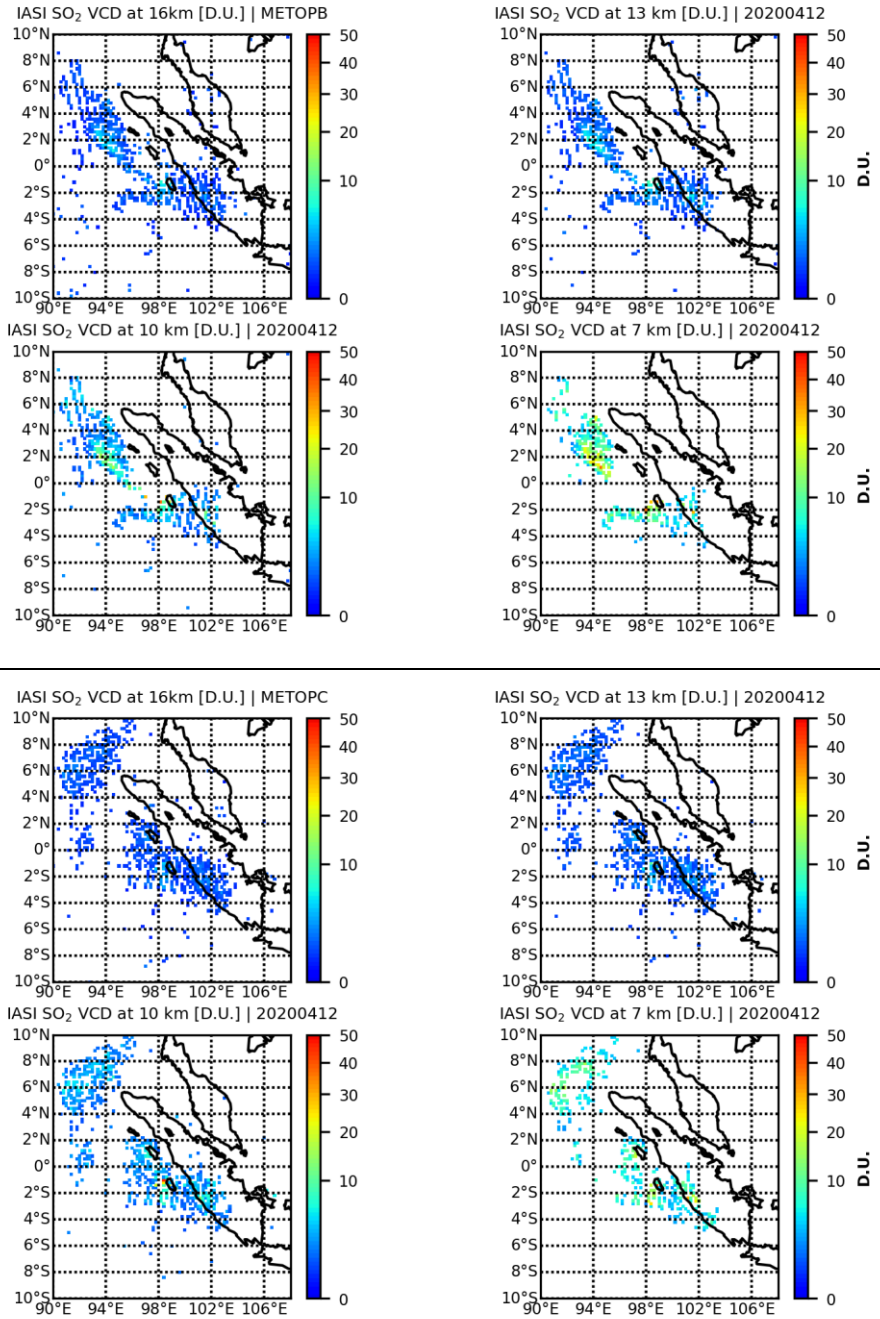

Figure 13. Example of the daily mean coverage of IASI-A [upper], IASI-B [middle] and IASI-C [lower] for the Anak Krakatau eruption on the 12th of April 2020. The multi-plots show the four reported SO_2 columns for 16 km [upper left], for 13 km [upper right], for 10 km [bottom left] and for 7 km [bottom right.] Gridded at 0.2x0.2°.

The scatter plots for the 3h common geographical points between IASI-C and IASI-A [upper] and IASI-B [lower] for the Anak Krakatau eruption, 11 to 13th of April 2020 are shown in **Figure 14**, same format as above, while the histogram representation of the differences are given in **Figure 15**. While the mean differences for all four SO_2 columns are approximately 0-1 D.U., the large standard deviations [between 3 and 12 D.U.] explain the relatively low correlations reported by the scatter plots. The amount of collocations to IASI-B [Table 3.5] is quite small, between 20 and 50.

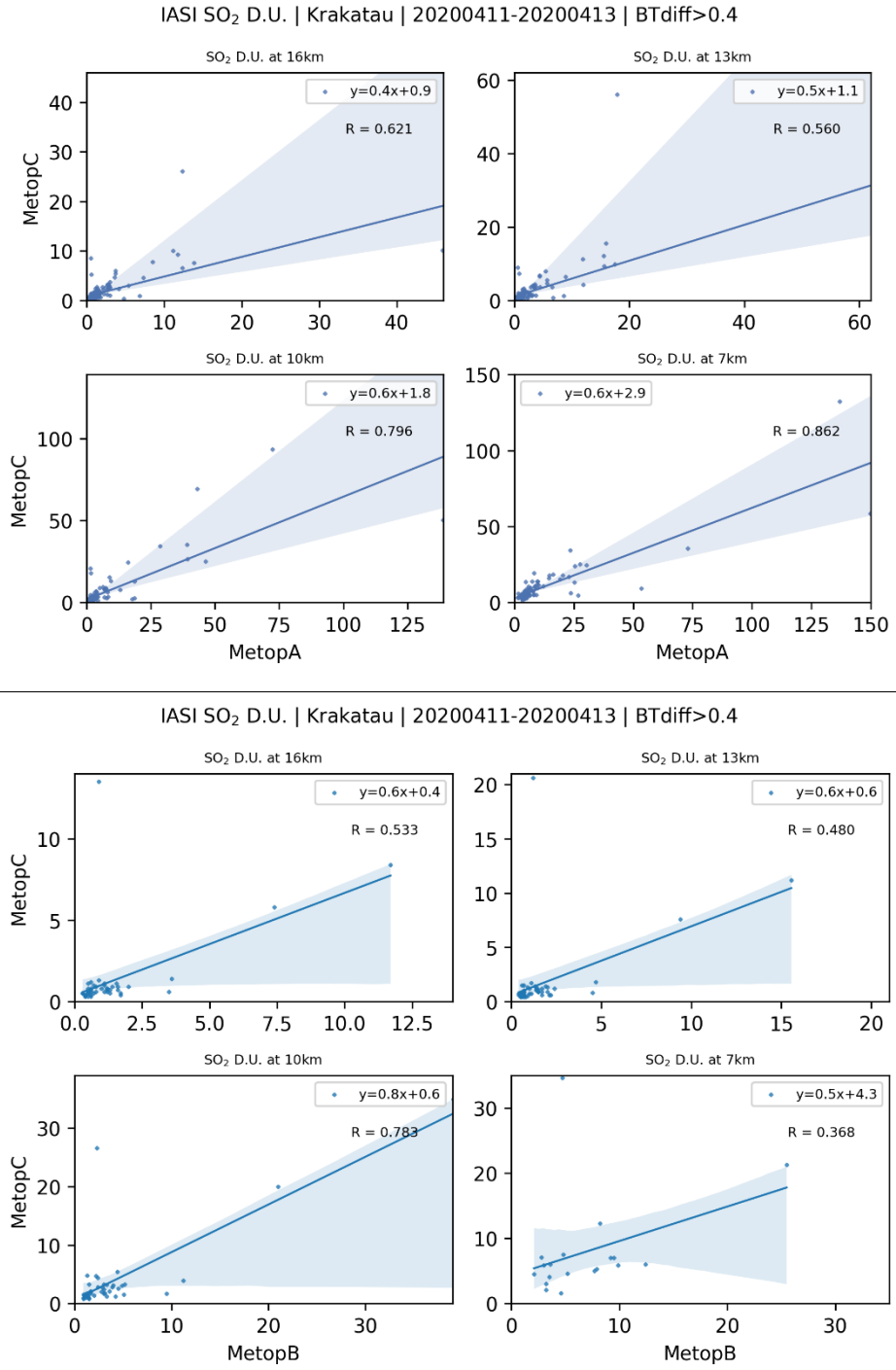

Figure 14. Scatter plots for the 3h common geographical points between IASI-C and IASI-A [upper] and IASI-B [lower] for the Anak Krakatau eruption, 11 to 13th of April 2020. The multi-plots show the four reported SO_2 columns for 16 km [upper left], for 13 km [upper right], for 10 km [bottom left] and for 7 km [bottom right.] Gridded at 0.2x0.2°.

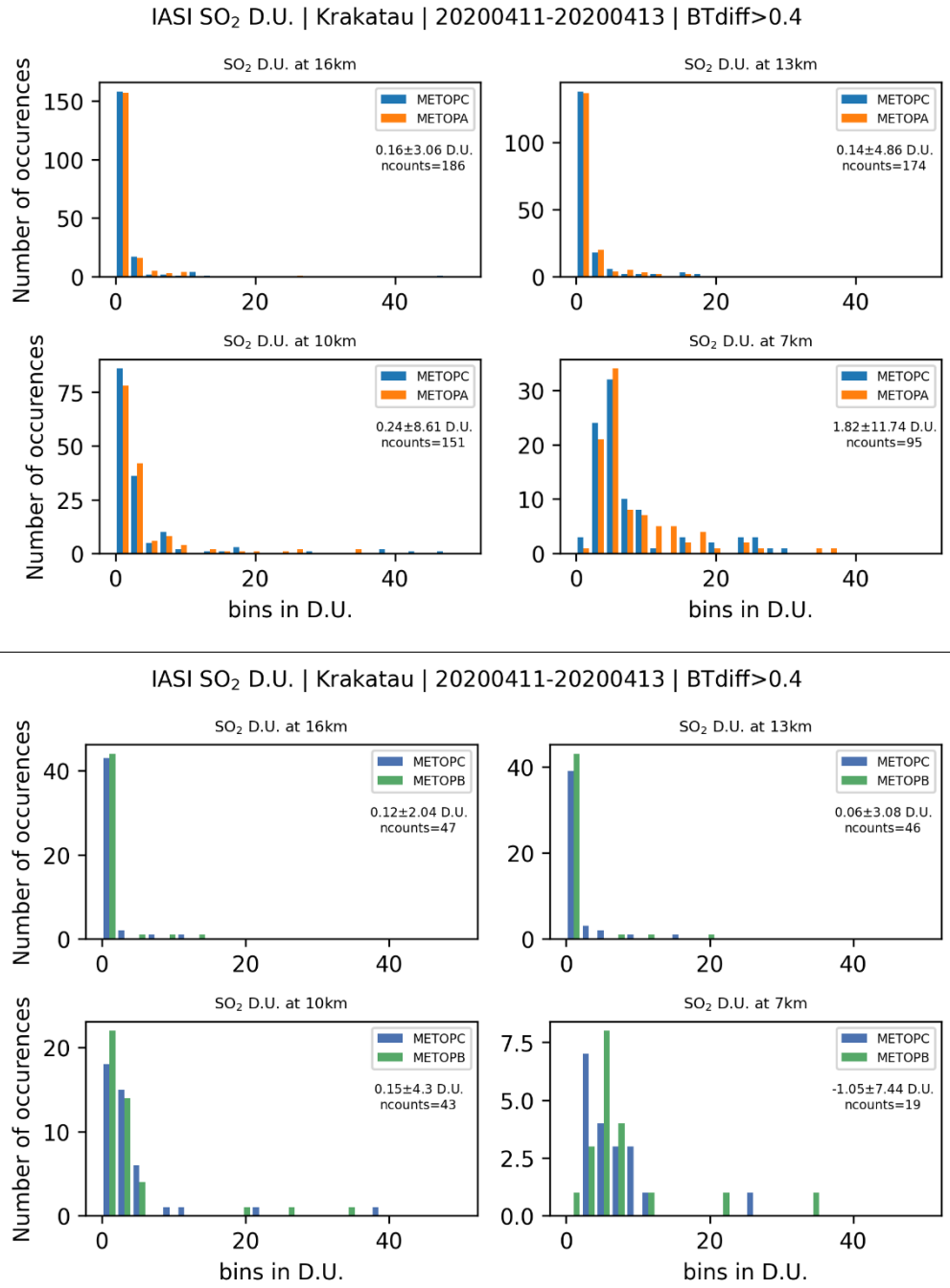

Figure 15. Histogram plots for the 3h common geographical points between IASI-C and IASI-A [upper] and IASI-B [lower] for the Anak Krakatau eruption, 11 to 13th of April 2020. The multi-plots show the four reported SO_2 columns for 16 km [upper left], for 13 km [upper right], for 10 km [bottom left] and for 7 km [bottom right.] Gridded at 0.2x0.2°.

Table 3.5 Mean difference, standard deviation and number of collocations for the Anak Krakatau eruption, 11 to 13th of April 2020.

IASI/MetopC	vs IASI/MetopA		vs IASI/MetopB	
Plume height	mean ± std	counts	mean ± std	counts
16km	0.16 ± 3.06 D.U.	186	0.12 ± 2.04 D.U.	47
13km	0.14 ± 4.86 D.U.	174	0.06 ± 3.08 D.U.	46
10km	0.24 ± 8.61 D.U.	151	0.15 ± 4.3 D.U.	43
7km	1.82 ± 11.74 D.U.	95	-1.05 ± 7.44 D.U.	19

Table 3.6. Slope, intercept and correlation coefficient for the Anak Krakatau eruption, 11 to 13th of April 2020, collocations.

IASI/MetopC	vs IASI/MetopA			vs IASI/MetopB		
Plume height	Slope	Intercept	R value	Slope	Intercept	R value
16km	0.397	0.852	0.621	0.628	0.387	0.533
13km	0.488	1.060	0.560	0.635	0.583	0.480
10km	0.627	1.821	0.796	0.816	0.617	0.783
7km	0.593	2.948	0.862	0.530	4.285	0.368

3.3 Nishinoshima, Japan | 20200704 to 20200724 – selected days

Selected days during the Nishinoshima, Japan, eruptive period of July-August 2020, are discussed in this report. In **Figure 16**, the daily mean coverage of IASI-A [upper], IASI-B [middle] and IASI-C [lower] for the Nishinoshima eruption, on the 4th of July 2020 is shown as example, in the same format as for previous eruptions. The equivalent scatter plots (**Figure 17**) and histogram plots (**Figure 18**) show that the mean difference is again ~0 D.U. with very small std levels (~1-2 D.U. for nearly all altitudes), while the low amount of collocations (Table 3.7 and Table 3.8) explain the non-optimal correlations.

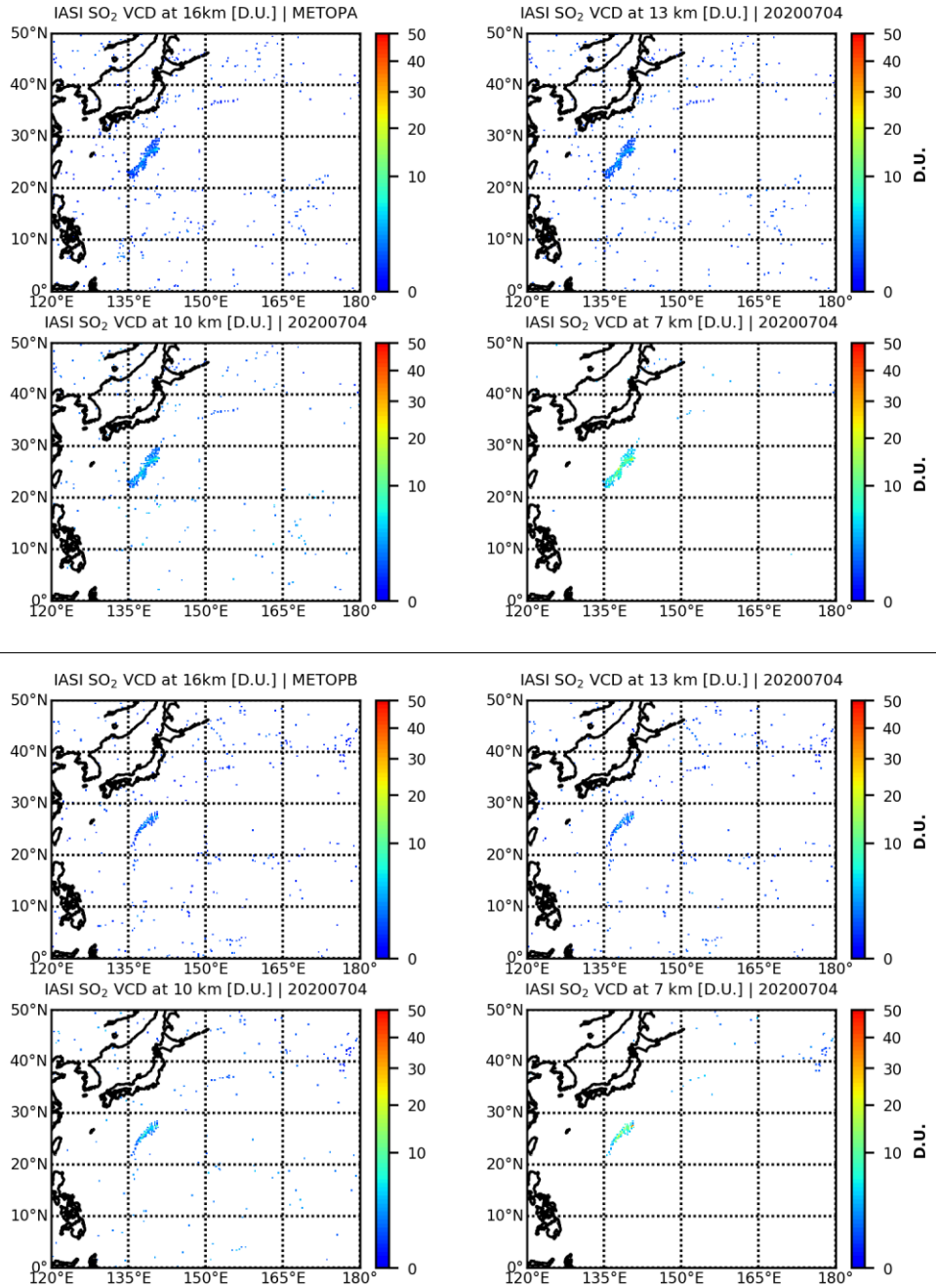

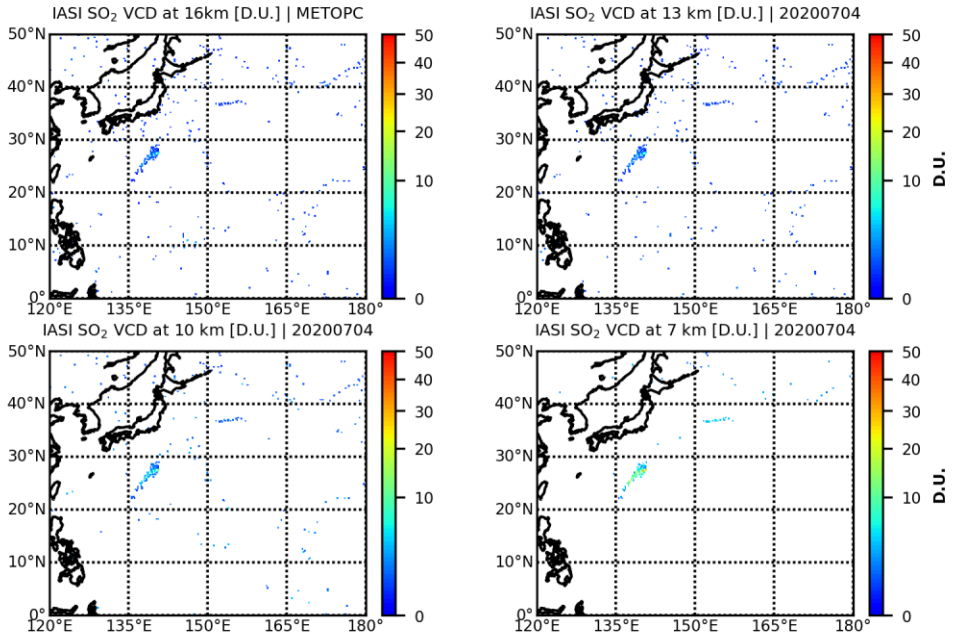

Figure 16. Example of the daily mean coverage of IASI-A [upper], IASI-B [middle] and IASI-C [lower] for the Nishinoshima eruption, on the 4th of July 2020. The multi-plots show the four reported SO_2 columns for 16 km [upper left], for 13 km [upper right], for 10 km [bottom left] and for 7 km [bottom right.] Gridded at 0.2x0.2°.

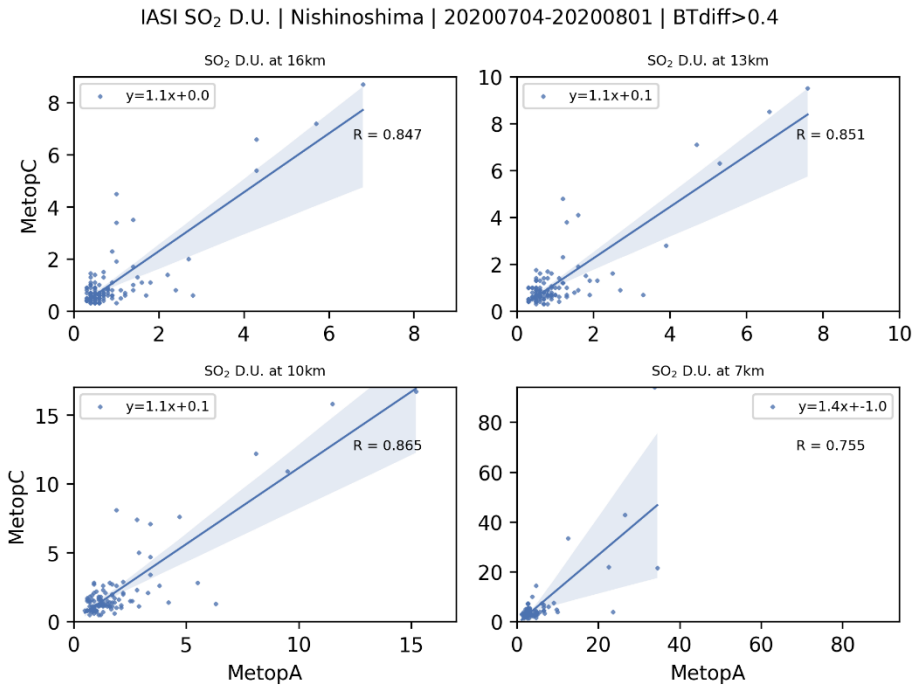

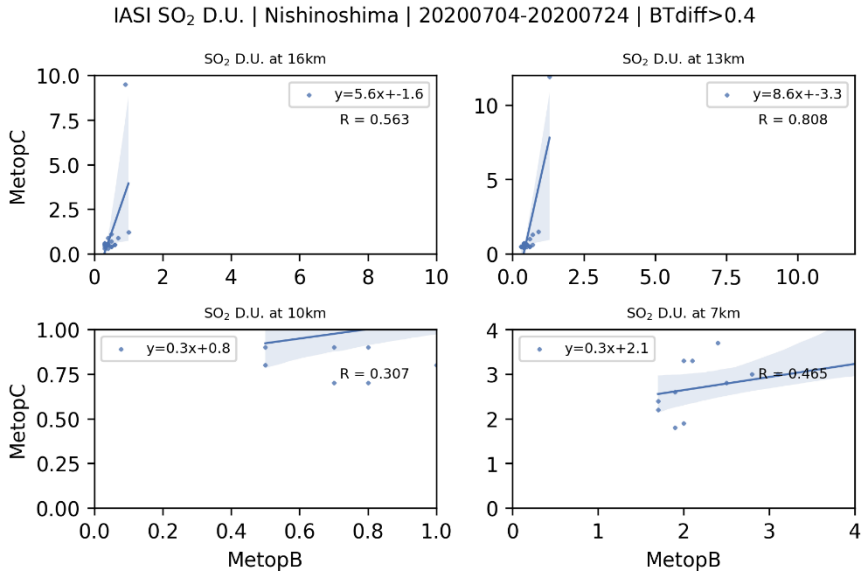

Figure 17. Scatter plots for the 3h common geographical points between IASI-C and IASI-A [upper] and IASI-B [lower] during the Nishinoshima eruptive period, 4th to 24th of July 2020. The multi-plots show the four reported SO_2 columns for 16 km [upper left], for 13 km [upper right], for 10 km [bottom left] and for 7 km [bottom right.] Gridded at 0.2x0.2°.

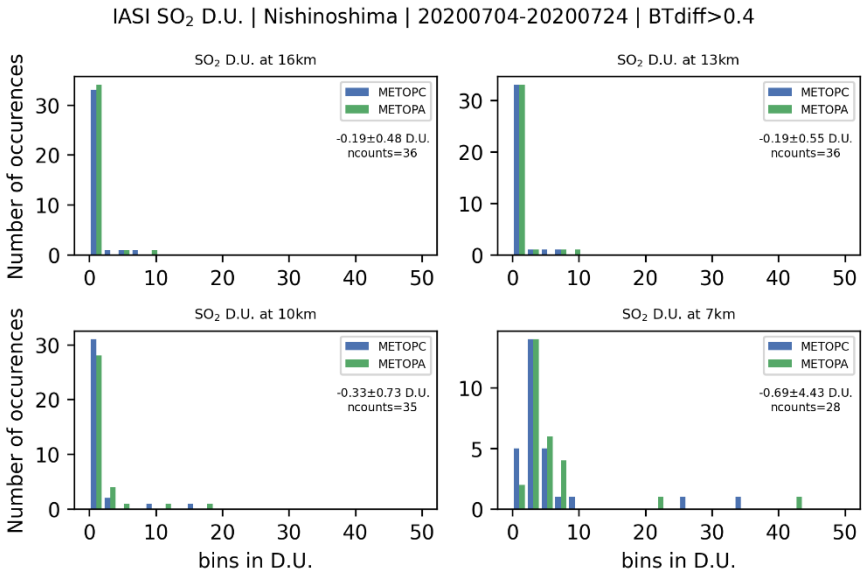

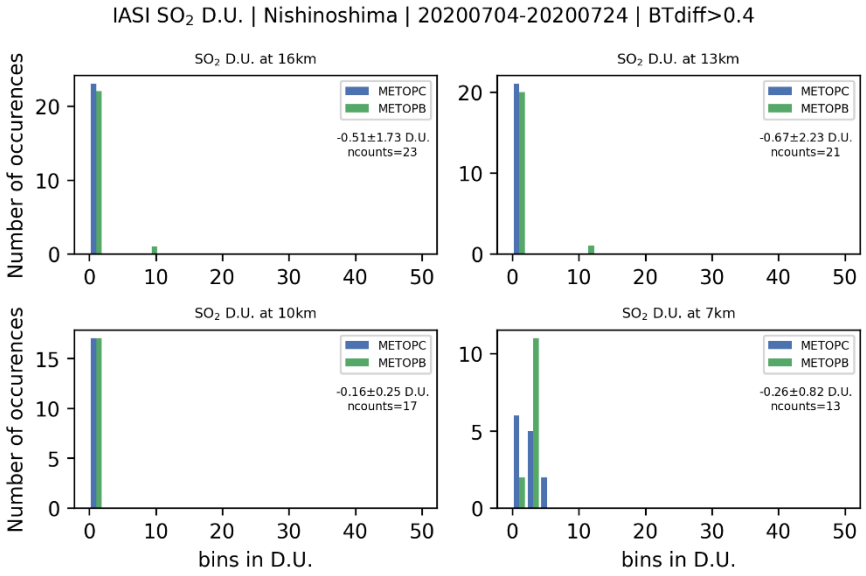

Figure 18. Histogram plots for the 3h common geographical points between IASI-C and IASI-A [upper] and IASI-B [lower] the Nishinoshima eruptive period, 4th to 24th of July 2020. The multi-plots show the four reported SO_2 columns for 16 km [upper left], for 13 km [upper right], for 10 km [bottom left] and for 7 km [bottom right.] Gridded at 0.2x0.2°.

Table 3.7 Mean difference, standard deviation and number of collocations for the Nishinoshima eruptive period, 4th to 24th of July 2020.

IASI/MetopC	**vs IASI/MetopA**		**vs IASI/MetopB**	
Plume height	mean ± std	counts	mean ± std	counts
16km	-0.19 ± 0.48D.U.	36	-0.51 ± 1.73D.U.	23
13km	-0.19 ± 0.55D.U.	36	-0.67 ± 2.23D.U.	21
10km	-0.33 ± 0.73D.U.	35	-0.16 ± 0.25D.U.	17
7km	-0.69 ± 4.43D.U.	28	-0.26 ± 0.82D.U.	13

Table 3.8. Slope, intercept and correlation coefficient for the Nishinoshima eruptive period, 4th to 24th of July 2020, collocations.

IASI/MetopC	**vs IASI/MetopA**			**vs IASI/MetopB**		
Plume height	Slope	Intercept	R value	Slope	Intercept	R value
16km	1.201	0.017	0.964	5.553	-1.610	0.563
13km	1.128	0.061	0.955	8.573	-3.336	0.808
10km	1.084	0.177	0.974	0.264	0.791	0.307
7km	0.918	1.117	0.837	0.293	2.056	0.465

3.4 Mt Etna, Sicily, Italy | 20210218 to 20210228

Mt Etna, Sicily, presented a series of eruptions during February and March 2021. As above, we fist present an example day for this eruption. In **Figure 19**, the daily mean coverage of IASI-A [upper], IASI-B [middle] and IASI-C [lower] on the 12th of February 2021 is shown as example, in the same format as for previous eruptions. The equivalent scatter plots (**Figure 20**) and histogram plots (**Figure 21**) show that the mean difference is again ~0 D.U. with very small std levels (~2-5 D.U. for nearly all altitudes), while the correlations, slopes and amount of collocations are shown in Table 3.9 and Table 3.10.

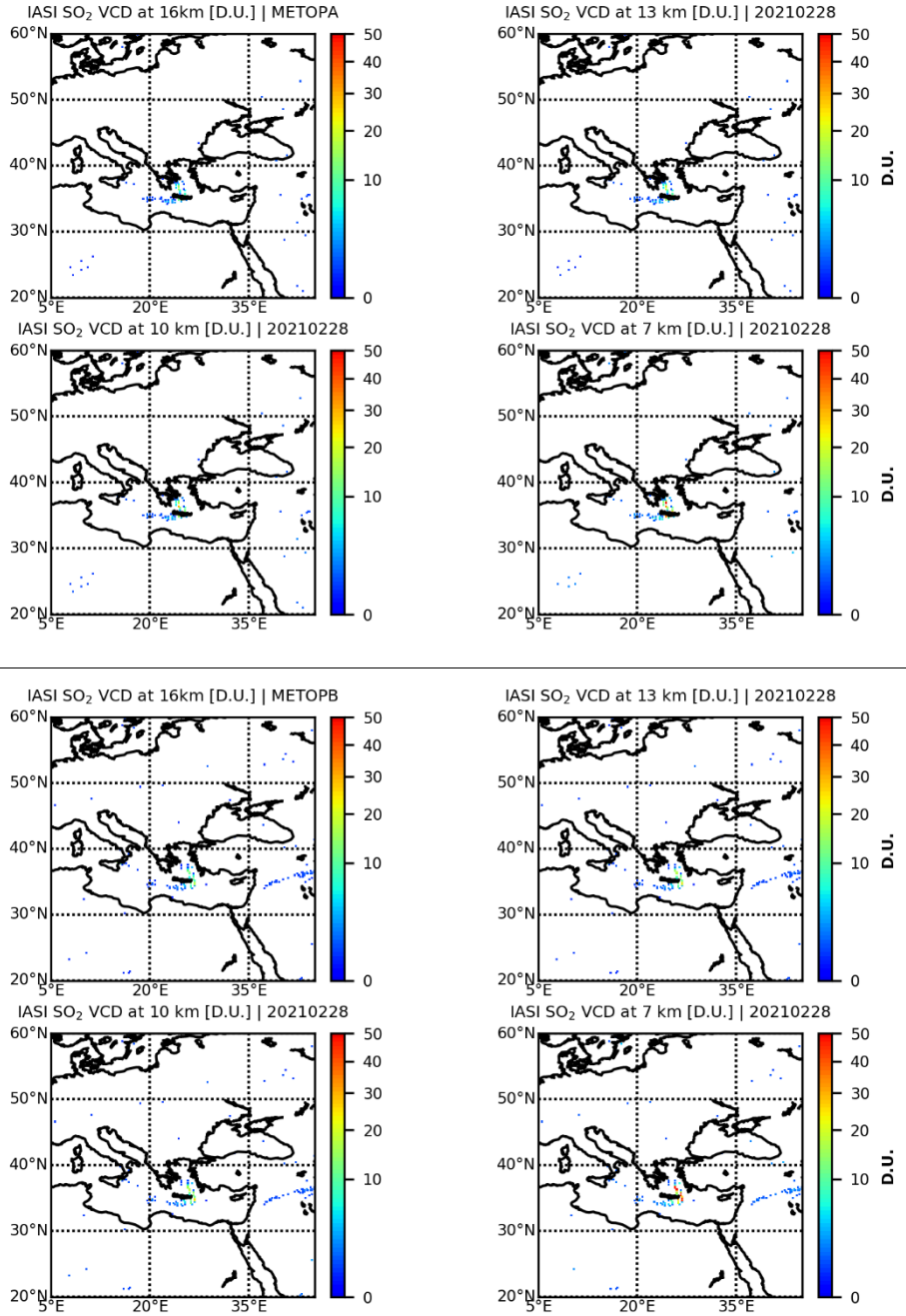

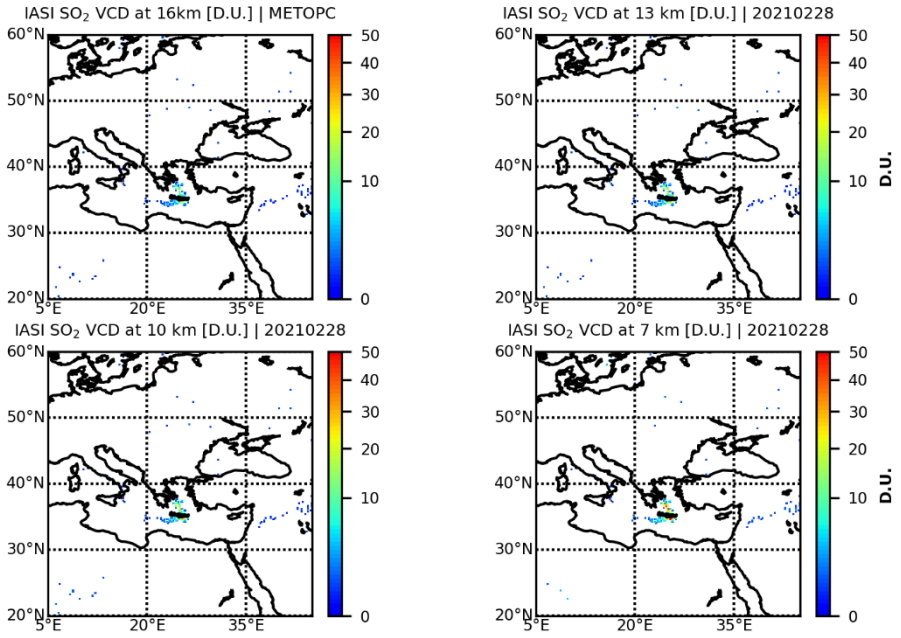

Figure 19. Example of the daily mean coverage of IASI-A [upper], IASI-B [middle] and IASI-C [lower] for the Mt Etna eruption on the 28th of February 2021. The multi-plots show the four reported SO_2 columns for 16 km [upper left], for 13 km [upper right], for 10 km [bottom left] and for 7 km [bottom right.] Gridded at 0.2x0.2°.

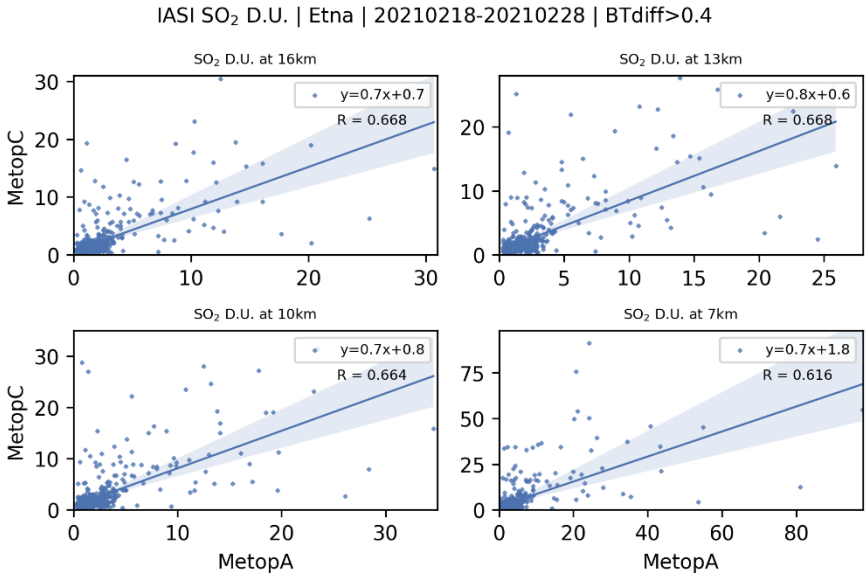

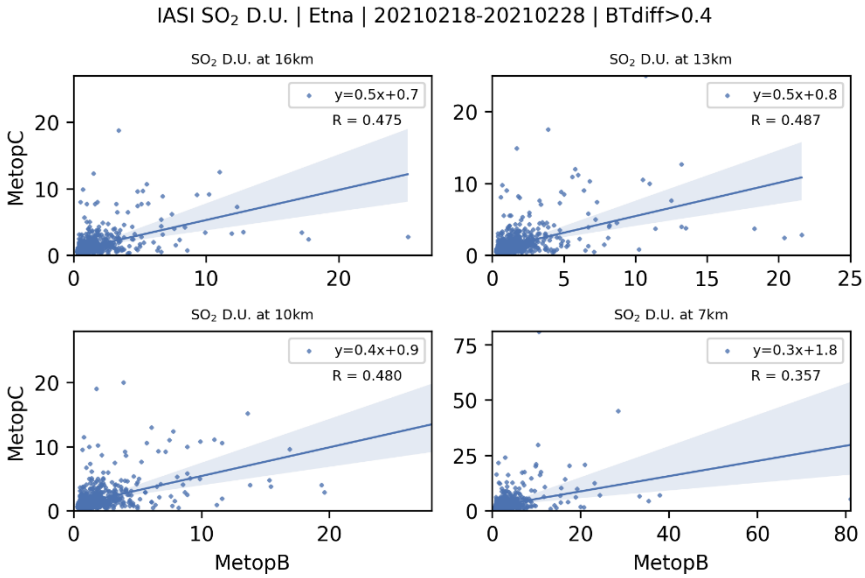

Figure 20. Scatter plots for the 3h common geographical points between IASI-C and IASI-A [upper] and IASI-B [lower] for the Mt Etna eruptive period between the 18th and the 28th of February 2021. The multi-plots show the four reported SO_2 columns for 16 km [upper left], for 13 km [upper right], for 10 km [bottom left] and for 7 km [bottom right.] Gridded at 0.2x0.2°.

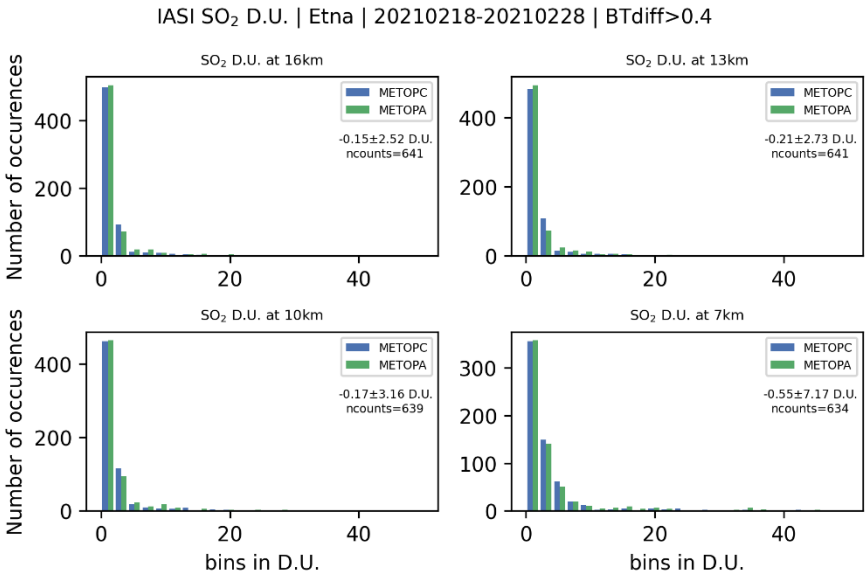

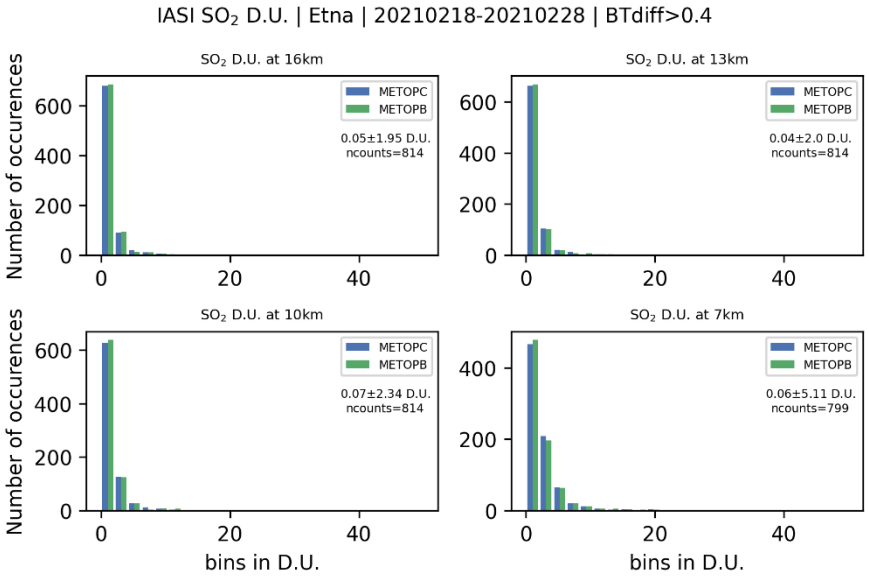

Figure 21. Histogram plots for the 3h common geographical points between IASI-C and IASI-A [upper] and IASI-B [lower] for the Mt Etna eruptive period between the 18th and the 28th of February 2021. The. The multi-plots show the four reported SO_2 columns for 16 km [upper left], for 13 km [upper right], for 10 km [bottom left] and for 7 km [bottom right.] Gridded at 0.2x0.2°.

Table 3.9 Mean difference, standard deviation and number of collocations for the Mt Etna eruptive period, 18 to 28th of February 2021.

IASI/MetopC	**vs IASI/MetopA**		**vs IASI/MetopB**	
Plume height	mean ± std	counts	mean ± std	counts
16km	-0.15 ± 2.52 D.U.	641	0.05±1.95D.U.	814
13km	-0.21 ± 2.73 D.U.	641	0.04±2.0D.U.	814
10km	-0.17 ± 3.16 D.U.	639	0.07±2.34D.U.	814
7km	-0.55 ± 7.17 D.U.	634	0.06±5.11D.U.	799

Table 3.10. Slope, intercept and correlation coefficient for the Mt Etna eruptive period, 18 to 28th of February 2021, collocations.

IASI/MetopC	**vs IASI/MetopA**			**vs IASI/MetopB**		
Plume height	Slope	Intercept	R value	Slope	Intercept	R value
16km	0.726	0.656	0.668	0.453	0.749	0.475
13km	0.778	0.647	0.668	0.464	0.797	0.487
10km	0.732	0.785	0.664	0.448	0.931	0.480
7km	0.684	1.772	0.616	0.343	1.847	0.357

4 CONCLUSIONS

In this report, we performed an inter-sensor validation by comparing the IASI/MetopC EUMETSAT NRT_PPF_v6.05 reported SO_2 columns against the ones reported by IASI/MetopA and IASI/MetopB for volcanic eruptions during the time line of the dataset, between September 2019 and March 2021. The SO_2 loads are reported at an assumed plume height at 7, 10, 13 ad 16km. The only filter on the datasets was that of the brightness temperature, which was restricted to be > 0.4K, as recommended. The retrieved SO_2 plume height is not delivered in this version of the datasets.

In order to mitigate the slightly different sensing times [~1h] between sensors, each day with volcanic signal was gridded at 3h intervals onto a 0.2x0.2° grid. For the major eruptive period of 13 to 19 of January 2020 over the Taal volcano, in the Philippines, we found a good collocation sample between IASI-C and IASI-A (IASI-B) between 7100 and 7800 common (4700 and 5300) grid points. The mean SO_2 load absolute difference for both comparisons was found to be 0.00 D.U. while the standard deviation increased slightly from 0.40 D.U. for the 16km plume to ~2.00 for the 7km plume. The linear correlations between IASI-C and IASI-A was also acceptable, between 0.77 and 0.83, however slightly reduced for the IASI-C to IASI-B comparisons [~0.78]. This led us to investigate whether decreasing the temporal criterion to 1h, instead of 3h, might improve these comparisons. Indeed, for the 1h comparisons, the statistics are entirely comparable for both comparative sets, with mean differences as previously, and correlations for both sensors and SO_2 altitudes at ~0.82.

The same, in principal, findings were shown for the Anak Karatau, Nishinoshima and Mt Etna, eruptions captured by the IASI instruments in the timeline of this report. In those cases however, the far smaller amount of collocations and highly varying volcanic plumes, resulted in higher standard deviations and slightly lower correlations, of similar order of magnitude between comparative datasets.

Overall, **we conclude that the IASI/MetopC SO_2 columns**, reported for different assumed plume altitudes, **are of the same quality as those of IASI/MetopA and IASI/MetopB** and are within the user requirements as stated in the Product Requirements Document [Table 1.1] and are reported **within the target accuracy of 100 % below 10 km and within the optimal accuracy of 50% above 10km.**

APPENDIX A.

Data descriptors of IASI Level 2 SO_2 BUFR file

DATA DESCRIPTOR		NAME USED HEREAFTER
0-0-1007	SATELLITE IDENTIFIER	
0-0-1031	IDENTIFICATION OF ORIGINATING/GENERATING CENTRE	
0-25-060	SOFTWARE IDENTIFICATION	
0-0-2019	SATELLITE INSTRUMENTS	
0-0-2020	SATELLITE CLASSIFICATION	
0-0-4001	YEAR	
0-0-4002	MONTH	
0-0-4003	DAY	
0-0-4004	HOUR	
0-0-4005	MINUTE	
0-0-4006	SECOND	
0-0-5040	ORBIT NUMBER	
0-0-5041	SCAN LINE NUMBER	
0-0-5001	LATITUDE (HIGH ACCURACY)	
0-0-6001	LONGITUDE (HIGH ACCURACY)	
0-0-5043	FIELD OF VIEW NUMBER	
0-0-7024	SATELLITE ZENITH ANGLE	
0-0-5021	BEARING OR AZIMUTH (DEGREE TRUE)	
0-0-7025	SOLAR ZENITH ANGLE	
0-0-5022	SOLAR AZIMUTH (DEGREE TRUE)	
0-0-7007	HEIGHT (Surface altitude in meter)	
0-4-0216	**GENERAL RETRIEVAL QUALITY FLAG FOR SO2**	**SO2_QFLAG**
0-1-5045	**SO2 COL ALTITUDE** (columns at different altitudes)	**SO2_COL_AT_ALTITUDES**
0-1-2080	**BRIGHTNESS TEMPERATURE REAL PART**	**SO2_BT_DIFFERENCE**
0-3-1001	**DELAYED DESCRIPTOR REPLICATION FACTOR (**Number of SO2 Levels NLSO2)	**number of altitudes=5**
0-0-7007	**HEIGHT**	**altitudes in m of the 5 altitudes levels**
0-0-7002	**HEIGHT OR ALTITUDE**	**SO2_ALTITUDE* (altitude of the plume)**
0-1-5045	**SULFUR DIOXIDE**	**SO2_COL* (total column)**

* Placeholders for future versions

APPENDIX B.

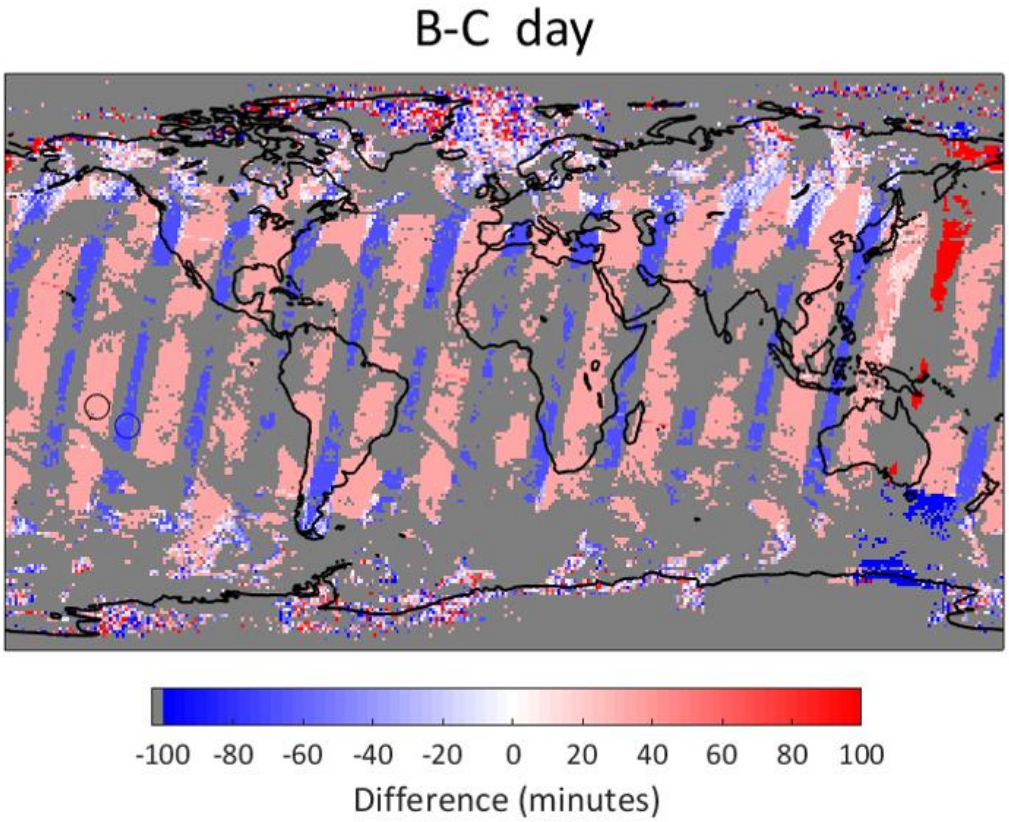

Figure 22. Temporal differences in sensing times for an entire day of orbits between IASI-B and IASI-C, in minutes.